Inhibition of the sarco/endoplasmic reticulum (ER) Ca^{2+}-ATPase by thapsigargin analogs induces cell death via ER Ca^{2+} depletion and the unfolded protein response

Received for publication, May 15, 2017, and in revised form, September 15, 2017 Published, Papers in Press, September 29, 2017, DOI 10.1074/jbc.M117.796920

Pankaj Sehgal[‡§¶1,2], Paula Szalai[‖1,3], Claus Olesen[‡¶], Helle A. Praetorius[‡], Poul Nissen[¶], Søren Brøgger Christensen[‡‡], Nikolai Engedal[‖4], and Jesper V. Møller[‡¶5]**

*From the [‡]Department of Biomedicine, Aarhus University, DK-8000 Aarhus, Denmark, [§]Biology Platform, Sunnybrook Research Institute, and Department of Biochemistry, University of Toronto, Toronto, Ontario M4N 3M5, Canada, [¶]Centre for Membrane Pumps in Cells and Disease (Pumpkin), Danish Research Foundation, DK-8000 Aarhus, Denmark, [‖]Centre for Molecular Medicine Norway (NCMM), Nordic European Molecular Biology Laboratory (EMBL) Partnership for Molecular Medicine, University of Oslo, P. O. Box 1137 Blindern, 0318 Oslo, Norway, **Danish Research Institute of Translational Neuroscience (DANDRITE), Nordic EMBL Partnership for Molecular Medicine, Department of Molecular Biology and Genetics, DK-8000 Aarhus, Denmark, and [‡‡]Department of Drug Design and Pharmacology, University of Copenhagen, DK-2100 Copenhagen, Denmark*

Edited by Roger J. Colbran

Calcium (Ca^{2+}) is a fundamental regulator of cell signaling and function. Thapsigargin (Tg) blocks the sarco/endoplasmic reticulum (ER) Ca^{2+}-ATPase (SERCA), disrupts Ca^{2+} homeostasis, and causes cell death. However, the exact mechanisms whereby SERCA inhibition induces cell death are incompletely understood. Here, we report that low (0.1 μM) concentrations of Tg and Tg analogs with various long-chain substitutions at the O-8 position extensively inhibit SERCA1a-mediated Ca^{2+} transport. We also found that, in both prostate and breast cancer cells, exposure to Tg or Tg analogs for 1 day caused extensive drainage of the ER Ca^{2+} stores. This Ca^{2+} depletion was followed by markedly reduced cell proliferation rates and morphological changes that developed over 2–4 days and culminated in cell death. Interestingly, these changes were not accompanied by bulk increases in cytosolic Ca^{2+} levels. Moreover, knockdown of two key store-operated Ca^{2+} entry (SOCE) components, Orai1 and STIM1, did not reduce Tg cytotoxicity, indicating that SOCE and Ca^{2+} entry are not critical for Tg-induced cell death. However, we observed a correlation between the abilities of Tg and Tg analogs to deplete ER Ca^{2+} stores and their detrimental effects on cell viability. Furthermore, caspase activation and cell death were associated with a sustained unfolded protein response. We conclude that ER Ca^{2+} drainage and sustained unfolded protein response activation are key for initiation of apoptosis at low concentrations of Tg and Tg analogs, whereas high cytosolic Ca^{2+} levels and SOCE are not required.

In addition to playing a key role in various cell-signaling processes, Ca^{2+} can be a potent inducer of cell death. The sarcoplasmic/endoplasmic reticulum Ca^{2+}-ATPase (SERCA),[6] present in endoplasmic reticulum (ER), serves a crucial role in Ca^{2+} homeostasis by maintaining a compartmentalized distribution of Ca^{2+} inside the cell. The high concentration in ER enables Ca^{2+} to exert its role as a regulator of various key cellular functions, *e.g.* muscle contraction and as a second messenger upon activation of $G\alpha_q$ coupled receptors. These events are based on the concerted function of Ca^{2+} channels in conjunction with the Ca^{2+}-transporting pumps that primarily are localized in the ER and plasma membrane (for a review, see Ref. 1).

Experimentally, specific effects of blocking SERCA activity can be conveniently studied with the aid of thapsigargin (Tg), a sesquiterpene lactone, the structure of which is shown in Fig. 1*A*. As a result of blocking SERCA pumps, Tg rapidly depletes ER Ca^{2+} stores. Although *per se* this effect only gives rise to transient and relatively slight (submicromolar) increases in intracellular Ca^{2+} concentration ($[Ca^{2+}]_i$) in non-muscle cells,

This work was supported by The Danish Council for Strategic Research (SPOT-Light) and from The Danish National Research Foundation (DNRF) to the Centre for Membrane Pumps in Cells and Disease (PUMPkin). The experiments performed at Sunnybrook Research Institute were supported by grants from the Canadian Institutes of Health Foundation (to David W. Andrews). The authors declare that they have no conflicts of interest with the contents of this article.

This article contains supplemental Figs. S1–S3 and Table S1.

[1] Both authors contributed equally to this work.

[2] Supported by DNRF and grants from The Lundbeck Foundation (to J. V. M.) and the Karen Elise Jensen Foundation (to C. O.).

[3] Supported by a grant from The Lundbeck Foundation (to P. N. and N. E.).

[4] To whom correspondence may be addressed: Centre for Molecular Medicine Norway (NCMM), Nordic EMBL Partnership for Molecular Medicine, University of Oslo, P. O. Box 1137 Blindern, 0318 Oslo, Norway. Tel.: 47-22840765; Fax: 47-22840598; E-mail: k.n.engedal@ncmm.uio.no.

[5] To whom correspondence may be addressed: Dept. of Biomedicine, Aarhus University, DK-8000 Aarhus, Denmark. Tel.: 45871-67754; E-mail: jvm@biomed.au.dk.

[6] The abbreviations used are: SERCA, sarcoplasmic/endoplasmic reticulum Ca^{2+}-ATPase; 8ADT, thapsigargin in which butyric acid has been replaced with 12-aminododecanoic acid at O-8; ATF4, activating transcription factor 4; BiP, heat shock 70-kDa protein 5 (glucose-regulated protein, 78 kDa); Boc-8ADT, *N-tert*-butoxycarbonyl-8ADT; $Ca_2E1/E2$, the two main conformations of Ca^{2+}-bound and Ca^{2+}-free SERCA, respectively; CHOP, DNA damage-inducible transcript 3; EpoTg, 7,11-epoxy derivative of thapsigargin; ER, endoplasmic reticulum; Grp94, glucose-regulated protein, 94 kDa; Orai1, calcium release-activated calcium channel protein 1; PSMA, prostate-specific membrane antigen; PSA, prostate-specific antigen; SOCE, store-operated Ca^{2+} entry; SR, sarcoplasmic reticulum; STIM, stromal interaction molecule; Tg, thapsigargin; UPR, unfolded protein response; TES, *N*-tris(hydroxymethyl)methyl-2-aminoethanesulfonic acid; Boc, *t*-butoxycarbonyl; PARP, poly(ADP-ribose) polymerase; HBS, HEPES-buffered saline; TBP, TATA-binding protein.

it has been suggested that depletion of Ca^{2+} from ER invokes a number of secondary events like the unfolded protein response (UPR) (2–5) and activation of store-operated Ca^{2+} entry (SOCE), flooding the cells with extracellular Ca^{2+} (6–8). Eventually, these events are considered to trigger cell death either by cytotoxicity arising from prolonged elevations of $[Ca^{2+}]_i$ (9–11) or a stress situation created by Ca^{2+} depletion from ER, leading to caspase activation and apoptosis (2–5). However, there is no consensus about the relative importance of these events for the apoptosis induced by Tg: whether it is Ca^{2+} depletion of ER or an increase in $[Ca^{2+}]_i$ that is decisive or whether both factors may, in fact, be important for an apoptotic outcome.

Interestingly, chemically modified analogs of Tg (12) are being used for antineoplastic purposes despite the general cellular toxicity of these compounds against both cancer and normal cells. The problem of toxicity in a therapeutic setting has been addressed by producing inactive prodrugs that can be activated by proteases to target specific cancer types (12, 13). With respect to prostate cancer, strategies have been designed to produce prodrugs that are transformed into active antineoplastic analogs upon proteolytic cleavage by prostate-specific antigen (PSA) (14, 15). This entails substituting the butanoate at O-8 in Tg (Fig. 1*A*) with 12-aminododecanoate to obtain a compound, 8ADT (Fig. 1*C*), that is useful for conjugation with a peptide cleavable by PSA (16). *In vivo* administration of this prodrug leads to extracellular formation of the lipophilic and cytotoxic Tg analog Leu-8ADT (Fig. 1*E*), which in contrast to the hydrophilic prodrug, is immediately taken up by the surrounding prostate cells, resulting in their demise (14). Another way of specifically targeting cancer cells with antineoplastic compounds is via formation of prodrugs activatable by prostate-specific membrane antigen (PSMA). PSMA is a proteolytic enzyme secreted by prostate cancers as well as by the neovascular endothelial cells of many solid tumors, *e.g.* those derived from kidney, breast, and bladder (13). Cleavage of the prodrug by PSMA also results in a 12-aminododecanoyl derivative of Tg, in this case βAsp-8ADT (Fig. 1*F*), as the active antineoplastic agent (13). This prodrug has been demonstrated to prolong the period of stable disease in the treatment of terminally ill patients with hepatocellular carcinoma resistant to sorafenib (17).

An important consideration for optimizing the drug effect is to know the exact mechanism by which the active component of the prodrug interacts with SERCA to induce cell death after the drug has been taken up by the cells. In the present investigation, we have studied how Tg and the 12-aminododecanoyl derivatives of Tg shown in Fig. 1 are bound to and affect SERCA function. Particularly interesting results were previously obtained with a Boc-protected derivative of 8ADT (Boc-8ADT; Fig. 1*D*), an analog with a strongly apoptotic effect similar to that of Tg (18). By X-ray studies, we could demonstrate that the Tg skeleton of the Boc analog is located in a binding pocket of SERCA1a that is formed among transmembrane helices 3, 5, and 7 in nearly the same way as Tg (19). Surprisingly, we observed that the long hydrophobic Boc-dodecanoyl side chain, by penetrating between the membrane helices of the ATPase, plunges deep into the membranous domain with the Boc group ending close to the putative N-terminal entrance for the Ca^{2+}-binding sites (20–22). Subsequently, we were able to establish traverse intercalation of membrane helices as a general mode of interaction for Tg analogs with long substituents at the O-8 position as shown in Fig. 1, *C–F*. This feature presumably is facilitated by the presence of a relatively open intramembranous pathway leading into the Ca^{2+} sites at the interior of the membrane domain (23). Although our ATPase inhibition data have been obtained on purified Ca^{2+}-ATPase from skeletal muscle (the SERCA1a isoform), this feature seems to be a general SERCA isoform property that correlates with the ability of the Tg analogs to induce apoptosis in cancer cells, which contain SERCA2b and -3 isoforms (24). However, we also found that although Boc-8ADT reacts very slowly with SERCA it exerts a stronger apoptotic effect in LNCaP cells than other O-8–substituted Tg analogs (18). Further *in vitro* experiments confirmed that Boc-8ADT binds slowly but with high affinity to SERCA (18). The question that arises from these experiments is to which degree the speed and affinity of analog-to-SERCA interaction is important for activation of the subsequent apoptotic effect.

In the present study, we have extended the initial observations and explored the effects of all the Tg analogs shown in Fig. 1 with respect to their interactions with SERCA and selected prostate and breast cancer cells. Our findings suggest that, rather than bulk changes in cytosolic Ca^{2+} concentration or SOCE, ER Ca^{2+} depletion and a sustained UPR play the major role in initiating the processes leading to cell death induced by Tg and the analogs.

Results

Interactions of thapsigargin analogs with SERCA

Inhibition of ATPase activity—The effect of the Tg analogs and Tg on Ca^{2+}-ATPase activity of purified SERCA1a was studied by a protocol that allows the measurement of both high affinity and kinetic aspects of the binding process after preincubation of the protein with gradually increasing inhibitor concentrations (Fig. 2). The first part of the Tg binding curve is linear (Fig. 2*A*) because it represents virtually complete binding of Tg to SERCA such that the activity decreases linearly with the added concentration of Tg and can be used to estimate the fraction of SERCA in the sample that is complexed by Tg. In the case of a Tg analog, higher concentrations than of Tg are required to produce equivalent reductions of activity due to lower affinities as demonstrated in Fig. 2*A* with Leu-8ADT and βAsp-8ADT as examples. The additional concentration of an analog needed to attain a given decrease in activity is a measure of the concentration of unbound analog required to give an equivalent binding of the analog to SERCA that like Tg is bound in a 1:1 complex to SERCA (23). This allows an estimate of K_d which is defined as the concentration of unbound inhibitor that gives rise to 50% decrease of activity during ATP hydrolysis. The results of these analyses are summarized in Table 1. They show that the inhibitors with amino acid O-8–substituted side chains bind to SERCA with K_d values in the 1–10 nM range. These values represent binding at high-affinity sites even

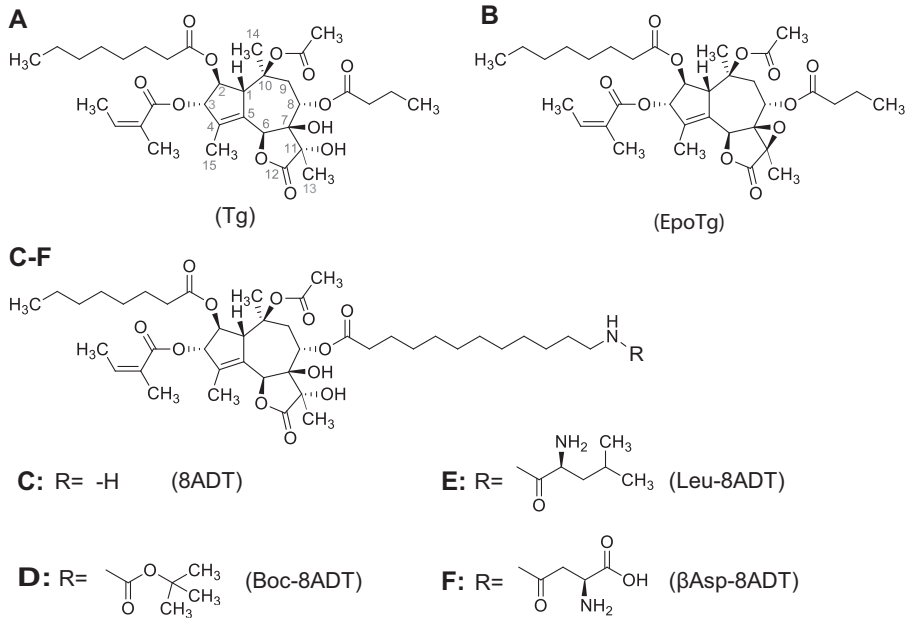

Figure 1. Constitutional formulae of Tg (*A*), EpoTg (*B*), and thapsigargin analogs in which the butanoyl group of thapsigargin at O-8 is substituted by 12-aminododecanoyl (8ADT; *C*) or the 12-amino group of 8ADT is blocked by Boc (Boc-8ADT; *D*) or terminates in Leu (Leu-8ADT; *E*) or βAsp (βAsp-8ADT; *F*).

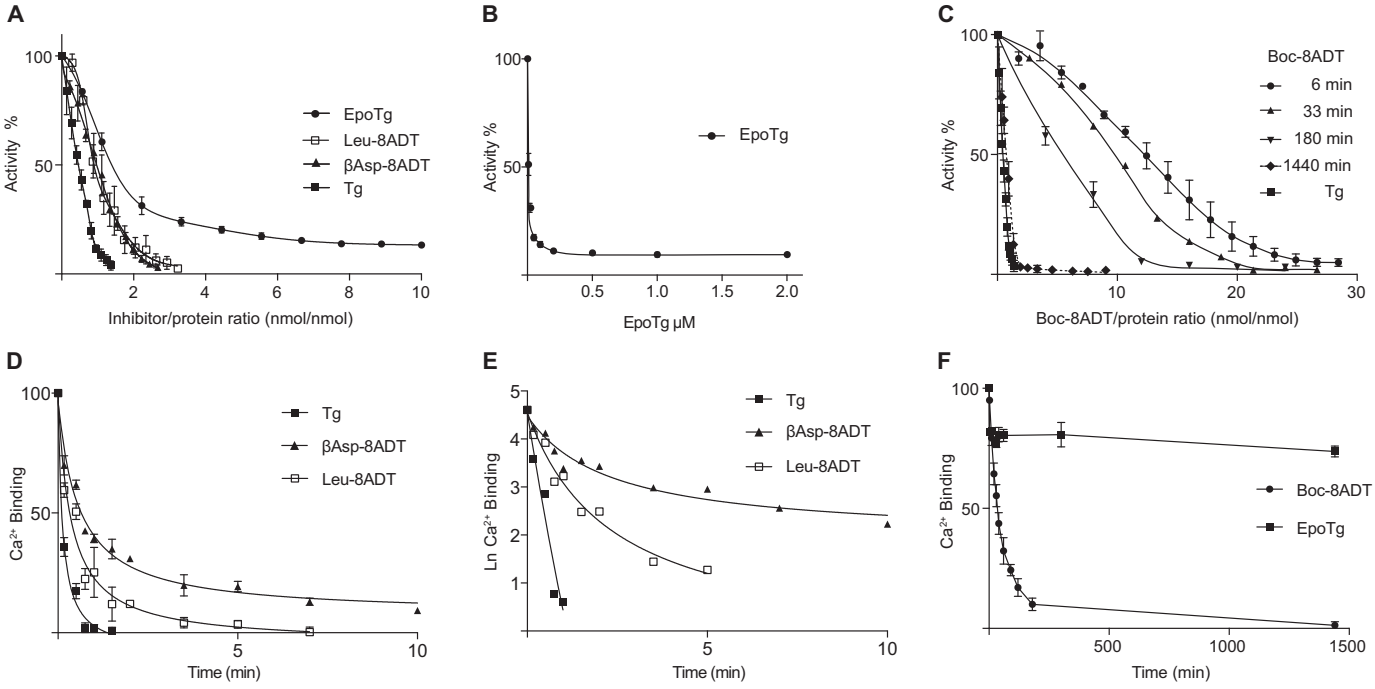

Figure 2. Inhibitory effects of Tg and Tg analogs on SERCA activity and removal of Ca^{2+} from the Ca_2E1 form of SERCA. *A–C*, inhibition of SERCA enzyme activity by Tg and Tg analogs. In *A* and *C*, activities were measured by sequential additions of Tg and Tg analogs in a titration type of experiment under conditions where a substantial fraction of the added inhibitors is bound to the ATPase due to their high affinity to SERCA (19). In *A*, the preincubation periods of inhibitor with SERCA before activity measurements were 3–6 min; in *C*, activities for Boc-8ADT were measured after 6, 33, 180, and 1440 min but otherwise following the same protocol as in *A*. *B* shows data for EpoTg, where in contrast to the O-8–substituted analogs a residual activity of 10 ± 1% persists at high (0.2–2 μM) concentrations. Note that, under these conditions in the presence of excess molar EpoTg, activities could be measured without recognizable error by direct addition to the enzymatic assay buffer. *D–F*, effects of addition of Tg and Tg analogs on the binding of Ca^{2+} to SERCA as a function of time. The experiments were conducted with SERCA at a protein concentration of 0.1 mg/ml in medium containing 50 mM MOPS (pH 7.2), 100 mM KCl, 5 mM Mg^{2+}, and 0.05 mM Ca^{2+} with labeled $^{45}Ca^{2+}$. Changes in Ca^{2+} binding were measured using double layers of Millipore filters after addition of 12 μM Tg, Leu-8ADT, βAsp-8ADT, Boc-8ADT, or EpoTg. *D* demonstrates the rapid Ca^{2+} release induced by Tg, βAsp-8ADT, or Leu-8ADT. *E* shows semilog plots of the changes in Ca^{2+} binding after addition of Tg, βAsp-8ADT, or Leu-8ADT. *F* shows data for Boc-8ADT and EpoTg measured over a period of 24 h. The experiments in each group comprise three to four experiments depicted in both non-logarithmic and semilog plots. *Error bars* of the non-logarithmic plots indicate S.D., the variability observed among individual experiments, whereas the curvature of the semilog data serves as an indicator of the rapid to slow kinetic transition as a function of time that in Table 1 is analyzed in terms of a biphasic reaction scheme.

Table 1

Concentration-dependent effects (K_d) of thapsigargin and analogs on SERCA ATPase activity and apparent Ca^{2+} dissociation rates from Ca_2E1–Inh (k_1) in the first step after binding of inhibitor and from CaE–Inh in the second step (k_2)

K_d values were calculated as described previously (23) and based on data from Fig. 2.

Compound	Inhibition	Ca^{2+} dissociation rate	
	K_d[a]	k_1[b]	k_2[b]
	nM	*min*$^{-1}$	
Tg[c]	0.2	2.5 ± 0.5[c]	2.5 ± 0.5
Leu-8ADT	7 ± 1	2.0 ± 0.3	0.55 ± 0.05
βAsp-8ADT	5 ± 1.5	2.3 ± 0.3	0.16 ± 0.01
Boc-8ADT[c]	4 ± 0.4	0.0215 ± 0.0001	0.0215 ± 0.0001
EpoTg	13 ± 1.5	0.0	0.0

[a] Concentration of free inhibitor required for 50% inhibition of Ca^{2+}-ATPase activity in 10 mM TES (pH 7.5), 100 mM KCl, 0.1 mM Ca^{2+}, 5 mM MgATP, 1 mM Mg^{2+} at 23 ± 0.2 °C. Based on data from Fig. 2.

[b] Apparent rate constants for the dissociation constants estimated from the release of the first and second bound Ca^{2+} in the presence of 12 μM Tg or Tg analogs. These rate constants ±S.D. were evaluated from double-exponential analysis of three experiments with well-resolved logarithmic data.

[c] Note that for Boc-8ADT and Tg, removal of both Ca^{2+} ions has been evaluated on the basis of a single reaction because kinetically k_1 and k_2 are not sufficiently well resolved to allow estimation of the individual apparent rate constants. For Boc-8ADT, K_d refers to the value obtained after 24-h preincubation.

though they are not nearly as strongly bound as Tg for which we have previously estimated the K_d to be around 0.2 nM (23).

Compared with Tg and the analogs mentioned above, the interaction of the 7,11-epoxy derivative of thapsigargin (EpoTg; Fig. 1*B*) and Boc-8ADT with SERCA is different. Although the apparent affinity of EpoTg for SERCA (K_d = 13 nM) according to these experiments is only slightly lower than that of the amino acid-containing analogs, a more important difference is that the inhibition of the activity at high EpoTg concentrations is incomplete, extrapolating to a retention of ATPase activity of 10 ± 1% (S.D.) relative to that of the inhibitor-free control at EpoTg concentrations of 0.2–2 μM (Fig. 2*B*).

Fig. 2*C* shows the effect of varying the preincubation time on the inhibition of the ATPase activity with Boc-8ADT. With 6 min of preincubation, the concentration-response relationship follows a sigmoid curve with little effect on enzyme activity up to concentrations that otherwise result in almost complete inhibition with the other Tg analogs. However, when the preincubation period is extended beyond 6 min, there is at every time-dependent step (33-, 180-, and 1440 min) an increase in the inhibitory effect accompanied by an approximation of the inhibition curve toward a hyperbolic reaction scheme. After 24-h incubation with Boc-8ADT, the K_d values are as low, or lower, than those observed with the other inhibitors (Table 1). In contrast, even if the preincubation period of the other analogs (including EpoTg) is similarly extended, there is no additional effect on inhibition beyond that taking place after 3–6 min (data not shown). The extended time scale thus shows that Boc-8ADT is also bound at equilibrium with high affinity, but with exceptionally slow kinetics.

Effects of thapsigargin analogs on Ca^{2+} release from SERCA—Ca^{2+} and Tg are considered to stabilize SERCA in each of the two major conformational states of the protein (Ca_2E1 and E2) according to an overall competitive reaction scheme: Ca_2E1 + Tg → E2–Tg + 2 Ca^{2+}. The basis for this is the essential structural difference between the E2 and E1 ATPase conformational states that only allows binding of Ca^{2+} at the two translocation sites in the E1 state. Fig. 2*D* shows that both Ca^{2+} ions are rapidly removed from SERCA by Tg, whereas within 1 min only one Ca^{2+} ion is dissociated from SERCA by Leu-8ADT and βAsp-8ADT. Dissociation of the second Ca^{2+} by the analogs is a slower process especially for βAsp-8ADT that requires several minutes (Fig. 2*D*). The biphasic character of the Ca^{2+} removal by the O-8–substituted analogs is demonstrated by the curved semilogarithmic plots shown in Fig. 2*E*, whereas for Tg, removal of both Ca^{2+} ions was too quick to resolve unequivocally the question of the monophasic or biphasic nature of the process.

Inspection and analysis of the semilogarithmic data for Leu-8ADT and βAsp-8ADT show that their mechanism of action is consistent with a sequential reaction scheme where first one Ca^{2+} is removed from Ca_2E1, accompanied by binding of the inhibitor, to form a Ca^{2+} plus inhibitor complex (CaE–Inh), which then in a following reaction involves the dissociation of the second bound Ca^{2+}, leading to the formation of an E2–Inh complex as shown by Reactions 1 and 2 below.

$$Ca_2E1 + Inh \rightarrow CaE\text{–}Inh + Ca^{2+}$$
Reaction 1

$$CaE\text{–}Inh \rightarrow E2\text{–}Inh + Ca^{2+}$$
Reaction 2

In this scheme, Reaction 1 represents the rapid removal of one bound Ca^{2+}, after instantaneous binding of inhibitor, to form CaE–Inh by dissociation of one Ca^{2+} followed by a slower removal of the second bound Ca^{2+} in Reaction 2 as shown by the apparent k_1 and k_2 rate constants given in Table 1 for Leu-8ADT and βAsp-8ADT. However, for Tg, both Ca^{2+} ions are rapidly removed with indistinguishable rate constants that are similar to k_1 for Leu-8ADT and βAsp-8ADT. Previous evidence suggests that a biphasic reaction scheme with different rate constants may nonetheless apply to the Tg-induced release of Ca^{2+} because the existence of a stable CaE–Tg intermediate has previously been demonstrated at a lower concentration of Tg (27).

In addition to the above mentioned kinetic scheme, we present below in Reactions 3 and 4 an alternative scheme according to which both Ca^{2+} ions can be removed before the inhibitor, in a slower step, reacts with the E2 form of SERCA to form the E2–Inh complex.

$$Ca_2E1 \rightarrow E2 + 2Ca^{2+}$$
Reaction 3

$$E2 + Inh \rightarrow E2\text{–}Inh$$
Reaction 4

This scheme is probably relevant for Boc-8ADT because the rate by which bound Ca^{2+} dissociates from Ca_2E1 in the presence of Boc-8ADT is very slow (Fig. 2*F* and Table 1), requiring 31.5 ± 1.5 min for conversion of 50% of Ca_2E1 to E2–Inh. This can be compared with the less than 1 min required for 50% conversion of Ca_2E1 to CaE–Inh with 12 μM Leu-8ADT or

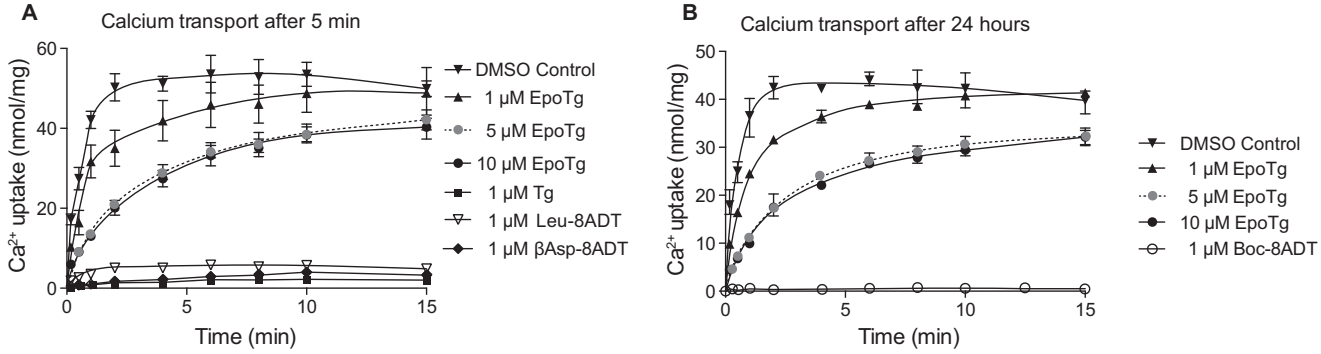

Figure 3. Effect of EpoTg on Ca^{2+} transport by SR vesicles as compared with that of Tg and O-8–substituted Tg analogs. SR vesicles (0.05 mg of protein/ml) were incubated at 23 ± 0.2 °C with medium containing 50 mM MOPS (pH 7.2), 100 mM KCl, and 5 mM Mg^{2+} together with 0.02 mM $^{45}Ca^{2+}$ and 0.1 mM EGTA buffer (with a pCa of ~6 to approach the low Ca^{2+} concentration inside a cell) in the absence (DMSO control) or presence of SERCA inhibitor as indicated. The reaction was started after 5 min (*A*) or 24 h (*B*) by addition of 0.08 mM MgATP to samples preincubated with no inhibitor (*inverted filled triangles*), 1 μM EpoTg (*upright filled triangles*), 5 μM EpoTg (*light gray circles*), 10 μM EpoTg (*black circles*), 1 μM Tg (*black squares*), 1 μM Leu-8ADT (*inverted empty triangles*), 1 μM βAsp-8ADT (*black diamonds*), or 1 μM Boc-8ADT (*empty circles*). Ca^{2+} accumulation by the vesicles was measured after timed intervals on 0.2-ml aliquots by addition of 4 ml of ice-cold incubation buffer and subsequent Millipore filtration. The plots represent the means of three to four experiments with S.D. *error bars* shown whenever appropriate, *i.e.* when the S.D. is of a greater magnitude than the size of the symbols.

βAsp-8ADT under otherwise similar conditions (Fig. 2*D* and Table 1).

As an additional feature, Fig. 2*F* shows that Ca^{2+} binding by EpoTg exhibits long-term stability. Immediately after addition of 12 μM EpoTg there is a modest (~15%) decrease of Ca^{2+} binding to SERCA, but thereafter the binding of Ca^{2+} remains constant as a function of time, even after 1 day (Fig. 2*F*). These data indicate that SERCA with bound EpoTg retains the ability to bind Ca^{2+} at both translocation sites, allowing some Ca^{2+}-ATPase activity to persist even at high EpoTg concentrations (Fig. 2*B*). In accordance with the latter findings, Fig. 3 shows that the activity retained in the presence of 1 μM EpoTg can be used to support Ca^{2+} accumulation in sarcoplasmic reticulum vesicles to the same extent, albeit at a slower rate than by DMSO control-treated sarcoplasmic reticulum vesicles. Even in the presence of very high concentrations of EpoTg (5 and 10 μM) we found that Ca^{2+} accumulates to about 80% of that observed in DMSO-treated vesicles after 15 min of measurement. As another notable feature, it can be seen that there is no difference between the uptake rates at 5 and 10 μM EpoTg. This observation probably indicates that the E1 form of SERCA at these high levels of EpoTg is saturated with EpoTg, forming transport-competent hybrid complex(es) with SERCA. In contrast, Ca^{2+} accumulation is totally inhibited by 1 μM Boc-8ADT after preincubation for 24 h (Fig. 3*B*), and this is also nearly the case after a 5 min preincubation with 1 μM Tg, βAsp-8ADT, or Leu-8ADT (Fig. 3*A*). This is in accordance with our finding that binding of these inhibitors to SERCA can exert a complete block in ATPase hydrolysis activity (Fig. 2, *A* and *C*).

Effects of thapsigargin and analogs on prostate and breast cancer cell function

Morphological effects and survival data—The effects of Tg and Tg analogs on SERCA1a prompted the second part of our study, which probed the effects of these compounds on various cancer cell lines. Previous investigations have indicated that the events leading to programmed cell death induced by Tg are slow and can be divided into two phases: an initial and potentially reversible phase, which ultimately ends with an "execution" phase and apoptosis (10). The survival data shown in supplemental Fig. S1 support the involvement of both phases, not only for Tg but also for the O-8–substituted analogs, in the prostate (LNCaP and PC3) and breast (MCF7) cancer cell lines tested. In these experiments, the cells were incubated with the inhibitors at a moderate (0.1 μM) concentration to follow the various phases leading to their death. For all cell lines and inhibitors, there was an increased cell density during the 1st day with continued but reduced proliferation rates before the second phase with definitive and deleterious changes that eventually resulted in cell death taking place in the following days. In our analysis, we measured changes in the number of surviving cells from manual cell counts recorded daily from the same selected fields of view. Both normal looking and affected cells were included in these counts. Affected cells were assumed to be viable if they were not dislodged from the culture plate surface and were without gross morphological abnormalities such as apoptotic-type cell shrinkage or appeared as necrotic fluid-imbibed ("ballooned") or as punctured, flat cells. In contrast, cells with a rounded and compact appearance were scored as affected but still living because they could regain normal morphology and replicative function after washout of inhibitor (data not shown). In most cases, the number of surviving cells declined at different rates after the first 1–2 days to reach complete extinction from the culture plates after 3–6 days. However, in a few instances, as noted below, cell densities stabilized at an almost constant level after the first days. When this occurred, there was evidence of decreased metabolic rates as indicated by a persisting red color of the phenol red in the medium, indicative of a reduced need for nutritional replacement of the medium.

Especially, the data for the LNCaP cells (supplemental Fig. S1A) demonstrated that Tg, Boc-8ADT, and Leu-8ADT were the most efficient compounds to induce morphological changes. This was observed after 1–2 days and was followed by gradual killing of the cells after 2–6 days with Boc-ADT and Tg being more efficient than Leu-8ADT. Conversely, 0.1 μM EpoTg did not cause any observable morphological changes,

and the cells proliferated at the same rate as the DMSO control. βAsp-8ADT and 8ADT exhibited an intermediary behavior: in the presence of these analogs, an increased cell density was also observed during the initial 1–2 days, but this was followed by no further changes or a slight decrease during the remaining observation period (supplemental Fig. S1A). In these stationary periods, nearly all the cells were morphologically changed after exposure to 0.1 μM βAsp-8ADT or 8ADT with no sign of cell death or metabolite exhaustion of the medium as noted above. Upon washout of inhibitor, the cells quickly recovered and proliferated to form confluent monolayers (data not shown). For the PC3 and MCF7 cells, the situation was quite different. In these cell lines, all cells (including those incubated with βAsp-8ADT and 8ADT) were dead after 6 days of incubation with a 0.1 μM concentration of the O-8–substituted analogs (supplemental Fig. S1, B and C). Cell death was preceded by reduced cell proliferation during the 1st day of exposure. All of the O-8–substituted inhibitors were about equipotent, whereas the appearance and proliferation rate of cells treated with 0.1 μM EpoTg were not changed compared with those of the DMSO control. Overall, massive cell death induction occurred more slowly in PC3 and MCF7 cells than in LNCaP cells.

To quantify concentration-dependent effects of Tg and the Tg analogs on cell proliferation and cell death at a larger scale and in an objective manner, we next used automated live-cell fluorescence microscopy (using an Essen Bioscience Incucyte instrument) in combination with propidium iodide as a marker of cells that have lost plasma membrane integrity. To compare the cytotoxic effects of the different Tg analogs, cell death was quantified after 60 (LNCaP) or 72 h (PC3 and MCF7) of treatment with a range of Tg or Tg analog concentrations and plotted relative to the maximal cell death levels obtained with Tg (Fig. 4). At these time points, more than 50% of the cells were dying/dead at maximally efficient Tg concentrations in all three cell lines (not shown). As evident in Fig. 4, all analogs induced cell death in a concentration-dependent manner, and at maximally efficient concentrations, the cytotoxic effect of all Tg analogs was similar to that obtained with maximal doses of Tg in all three cell lines. However, the concentration required to obtain maximal cell death varied substantially among the different analogs. To quantify the differences, dose-response curves such as those shown in Fig. 4 were used to calculate "$LD_{50(Tg\text{-}max)}$" values, defined as the inhibitor concentration required to obtain 50% of the maximal Tg response (Fig. 4, values indicated below the *x axes*). When matching $LD_{50(Tg\text{-}max)}$ values for Tg and individual Tg analogs across the three cell lines, we found that PC3 cells had slightly lower or similar $LD_{50(Tg\text{-}max)}$ values compared with MCF7 cells (0.8–1.9-fold difference compared with PC3 cells where among the Tg analogs only EpoTg showed a lower $LD_{50(Tg\text{-}max)}$ in MCF7 cells), whereas LNCaP cells had much higher $LD_{50(Tg\text{-}max)}$ values (6–20-fold higher $LD_{50(Tg\text{-}max)}$ values compared with those observed in PC3 cells). When comparing the cytotoxic actions of the various Tg analogs, Boc-8ADT and Leu-8ADT were found to be the two most potent inducers of cell death in all cell lines with Boc-8ADT showing $LD_{50(Tg\text{-}max)}$ values that were 10–20% lower (LNCaP and PC3) or 1.6-fold higher (MCF7) than those observed with Tg itself and Leu-8ADT showing $LD_{50(Tg\text{-}max)}$ values that were 1.4–4.6-fold higher than those observed with Tg (Fig. 4). βAsp-8ADT was less potent than Boc-8ADT and Leu-8ADT in all three cell lines, displaying 5–13-fold higher $LD_{50(Tg\text{-}max)}$ values than those obtained with Tg (Fig. 4). Finally, EpoTg was clearly much less potent than the O-8–substituted analogs in all three cell lines because 129–167-fold higher concentrations of EpoTg were required to obtain the same degree of cytotoxicity as that observed with Tg (Fig. 4).

To substantiate these findings as well as to assess potential selective effects of Tg and Tg analogs on cell proliferation, overall cell densities (as calculated by the software algorithm of the Incucyte instrument) were followed over time (supplemental Fig. S2) in the same experiments as described above. Overall, for all SERCA inhibitors and in all three cell lines, loss of cell density correlated very well with increases in cell death (compare graphs in supplemental Fig. S2 with Fig. 4). Interestingly, however, we frequently observed concentrations of Tg and Tg analogs at which the increase in cell density was halted but without concomitant induction of cell death (supplemental Fig. S2 and Fig. 4; compare for example the effects of 6 nM Tg, 25 nM Leu-8ADT, or 2500 nM EpoTg in LNCaP cells or 8 nM βAsp-8ADT in MCF7 cells) or visible morphological changes (not shown). The concentration window where such intermediate but still selective antiproliferative effects could be observed was quite narrow, and within the concentration ranges tested in our experiments, it was more readily detectable in LNCaP and MCF7 cells compared with PC3 cells.

Cell $[Ca^{2+}]_i$ measurements and the role of SOCE in Tg-induced cell death—To probe how the cellular effects of Tg and the analogs are correlated with their properties as SERCA inhibitors, we also studied their effects on cellular Ca^{2+} homeostasis. In short-term experiments, this was done by observing the immediate effects of exposing Fluo-4-AM-loaded cells to a 1 μM concentration of the SERCA inhibitors. The cells were transferred to a modified Hanks' medium that contained 1 mM EGTA to avoid Ca^{2+} uptake from the medium. Representative traces obtained from PC3 and LNCaP cells are shown in Fig. 5. In both cell lines, exposure to 1 μM Tg resulted in a sharp rise in $[Ca^{2+}]_i$ followed by a gradual decline toward the same baseline values of $[Ca^{2+}]_i$ as before the Tg addition. This is consistent with depletion of Ca^{2+} from the ER stores and subsequent removal from the cytosolic compartment either by transport out of the cell or by uptake in other cellular organelles like mitochondria and the Golgi apparatus.

Interestingly, exposure of PC3 and LNCaP cells to 1 μM βAsp-8ADT or Leu-8ADT consistently gave rise to a delayed response with broader and flatter peaks compared with those obtained with Tg (Fig. 5 and supplemental Table S1). As shown in supplemental Table S1, the delay times for βAsp-8ADT and Leu-8ADT were 6.2 ± 1.3 and 10.5 ± 2.4 min, respectively, in PC3 cells (mean values ±S.D. from five experiments), whereas the delay times were 13.8 ± 3.9 and 24.4 ± 2.9 min in LNCaP cells (mean values ±S.D. from three experiments). The delay times were thus about twice as long in LNCaP compared with PC3 cells and longer for Leu-8ADT compared with βAsp-8ADT. We also observed a delayed response with EpoTg, but with this analog the delay was less pronounced than with βAsp-8ADT and Leu-8ADT, especially in PC3 cells (supplemental Table S1; EpoTg

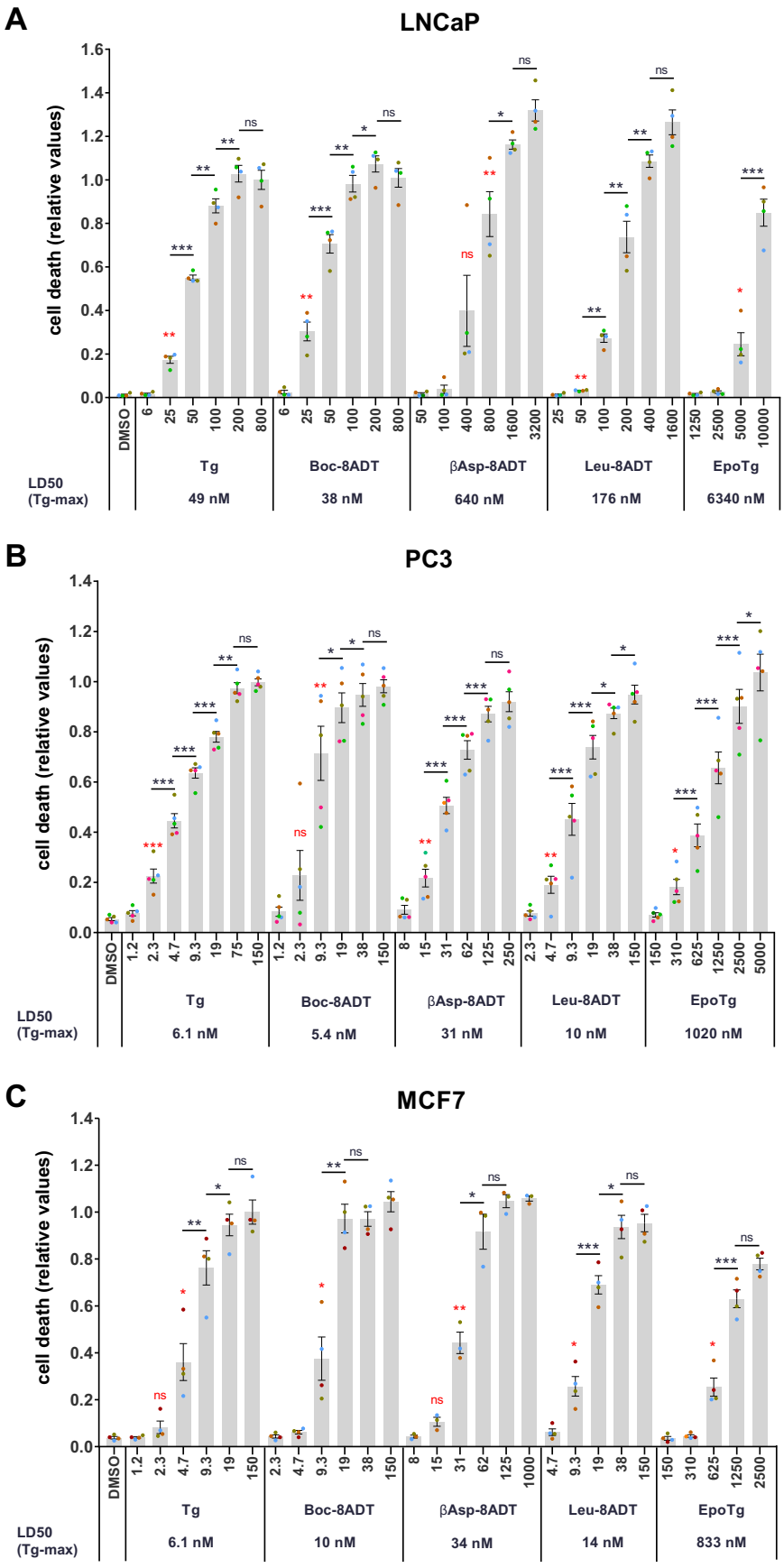
A
LNCaP
cell death (relative values)
Tg
Boc-8ADT
βAsp-8ADT
Leu-8ADT
EpoTg
LD50 (Tg-max)
49 nM
38 nM
640 nM
176 nM
6340 nM
B
PC3
6.1 nM
5.4 nM
31 nM
10 nM
1020 nM
C
MCF7
6.1 nM
10 nM
34 nM
14 nM
833 nM

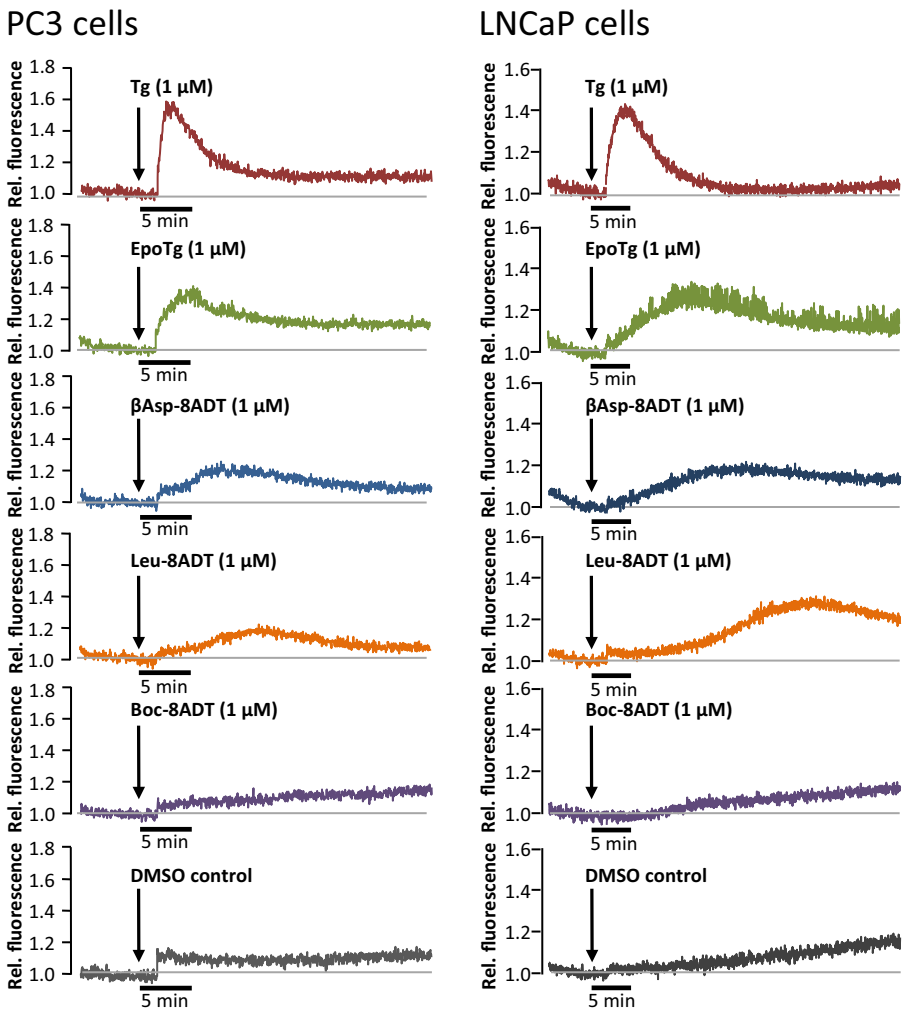

Figure 5. Effect of Tg and Tg analogs on the release of Ca^{2+} from the ER to the cytosol of prostate cancer cells. PC3 (*left panels*) and LNCaP cells (*right panels*) were seeded in polylysine-coated plates and loaded with Fluo-4-AM in Ca^{2+}-containing HBS medium before being exposed to 1 μM concentrations of Tg, EpoTg, βAsp-8ADT, Leu-8ADT, Boc-8ADT, or DMSO control (0.1%) solubilized in a nominally Ca^{2+}-free HBS containing 1 mM EGTA. Fluorescence traces were recorded at 535 nm after excitation of the cells at 488 nm. The result from one representative experiment of five (PC3) or three (LNCaP) independent experiments is shown (see also supplemental Table S1 for a quantitative comparison of the effects of EpoTg, βAsp-8ADT, and Leu-8ADT relative to Tg).

delay time, 2.1 ± 0.4 min in PC3 cells and 8.5 ± 3.2 min in LNCaP cells). Evidently, LNCaP cells respond markedly more slowly to the Tg analogs EpoTg, βAsp-8ADT, and Leu-8ADT than PC3 cells (notice also the different time scales used to depict the PC3 and LNCaP data in Fig. 5). In contrast to Tg and the above mentioned Tg analogs, Boc-8ADT did not induce any changes in $[Ca^{2+}]_i$ in this or any other short-term experiments, including those performed with MCF7 cells (Fig. 5 and data not shown). We consider it likely that the long delays and slender fluorescent peaks observed with the above mentioned analogs, at least in part, reflect retarded passage of the analogs across the outer cell membrane as compared with Tg. This may for βAsp-8ADT and Leu-8ADT be attributed to the increased hydrophobicity imparted by the O-8–dodecanoyl linker, which by increased interaction with membrane lipids (23) is likely to impede the passage of these analogs into the cells. Differences due to electrostatic effects caused by the additional negative charge that is present in βAsp-8ADT are also possible. By contrast, the absence of any measurable effect of Boc-8ADT can be attributed to the very slow interaction of this analog with

Figure 4. Dose-dependent cell death induction by Tg and Tg analogs in LNCaP, PC3, and MCF7 cells. LNCaP (*A*), PC3 (*B*), or MCF7 (*C*) cells were seeded in 96-well plates and incubated for 2 days. Subsequently, the cells were treated with 0.1% DMSO control or the indicated concentrations (in nM) of Tg, Boc-8ADT, βAsp-8ADT, Leu-8ADT, or EpoTg together with 2.5 μg/ml propidium iodide in complete medium. Cell death was assessed using an Incucyte instrument for automated live-cell imaging and calculation of red fluorescence and total cell confluence. Cell death is plotted as the ratio of red fluorescence to total cell confluence after 60 (*A*) or 72 h (*B* and *C*) normalized to the highest cell death level obtained with Tg. $LD_{50(Tgmax)}$ values, defined as the Tg/Tg analog concentration required to obtain 50% of the maximal Tg response, are indicated below the *x axis* denominators. Data are means ± S.E. from four (LNCaP and MCF7) or five (PC3) independent experiments with *error bars* representing S.E. Single points represent individual measurements (mean values from triplicate wells), and each experiment is indicated with differently colored points. *Red asterisks*, paired Student's *t* test compared with DMSO control to indicate the lowest concentration of Tg/Tg analog that significantly increases cell death. Paired Student's *t* tests comparing each subsequent stepwise increase in Tg/Tg analog concentration are indicated with *black bars* between each compared condition and with *black asterisks* to indicate significance levels. *, $p < 0.05$; **, $p < 0.01$; ***, $p < 0.001$; *ns*, not significant (*i.e.* $p \geq 0.05$).

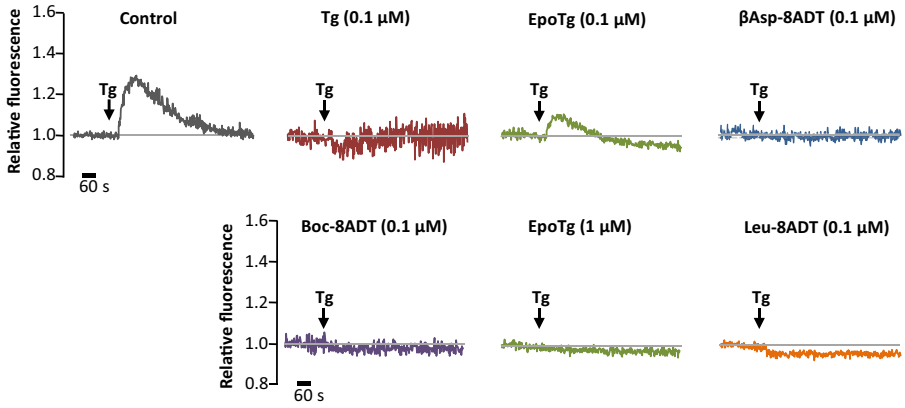

Figure 6. ER Ca^{2+} depletion of PC3 cells after preincubation with Tg or Tg analogs. PC3 cells were seeded in standard growth medium and exposed for 24 h to 0.1 μM or 1 μM concentrations of Tg or Tg analogs as indicated prior to loading with Fluo-4-AM. Thereafter, the medium was switched to 1 mM EGTA in HBS and supplemented after 10 min with 1 μM Tg (indicated by *arrows*) to release any Ca^{2+} remaining in the Tg-sensitive Ca^{2+} stores in the cell. Note that ER (*i.e.* Tg-sensitive) Ca^{2+} release could only be observed from the 0.1 μM EpoTg-pretreated cells and from the DMSO control cells that had not been pretreated with inhibitor. One representative experiment of four is shown. In these four experiments, the amplitudes related to the Ca^{2+} eluted with the Tg purge in the 0.1 μM EpoTg-pretreated cells varied from 30 to 55% of that eluted with Tg from the DMSO control cells.

SERCA (Fig. 2*C*), whereas the absence of a dodecanoyl linker in EpoTg likely gives more ready access of this analog to the cell interior, which, at least in part, can explain the faster Ca^{2+} effect of this analog compared with βAsp-8ADT and Leu-8ADT in cells.

In another set of experiments, we evaluated the effect of the SERCA inhibitors on the Ca^{2+} content of the ER in PC3 cells that had been preincubated with the inhibitors in normal growth medium for 24 h (Fig. 6). Before the measurements, the cells were loaded with Fluo-4-AM followed by perfusion for 10 min with modified Hanks' medium (containing 1 mM EGTA) and 1 μM Tg to provide a purge for Ca^{2+} that might have remained in the ER after the 24 h pretreatment. Interestingly, we found that after pretreatment with 0.1 μM Tg or O-8–substituted analogs PC3 cells did not respond to the Tg purge with an efflux of Ca^{2+} (Fig. 6). In contrast to this, Ca^{2+} release from the ER could, as expected, be readily registered in control cells that had only been exposed to DMSO during the 24-h pretreatment period. Ca^{2+} was partly retained in the ER stores after pretreatment with 0.1 μM EpoTg (which is nontoxic in PC3 cells), whereas a 24 h pretreatment with 1 μM EpoTg (which is lethal in PC3 cells) was sufficient to prevent a detectable release of Ca^{2+} from the ER to the cytosol upon subsequent exposure to Tg (Fig. 6). Thus, the partial depletion of ER Ca^{2+} content that we observed after 1 day of exposure to 0.1 μM EpoTg (Fig. 6) did not affect cell proliferation or viability (supplemental Fig. S1B and Fig. 4*B*). In contrast, the very efficient depletion of ER Ca^{2+} content that was observed with a 0.1 μM concentration of O-8–substituted analogs or 1 μM EpoTg (Fig. 6) was associated with a massive decline in cell proliferation (supplemental Figs. S1B and S2B) and cell death (Fig. 4*B*). Notably, the inability of Tg to release ER Ca^{2+} after pretreatment with a 0.1 μM concentration of O-8–substituted analogs or with 1 μM EpoTg was not due to an inability of Tg to bind and block SERCA because EpoTg and the other analogs have considerably lower affinities for SERCA than Tg (Table 1) and because the majority of the analogs, including EpoTg, was washed out before the Tg purge. Additionally, the Ca^{2+} ionophore A23187 was virtually unable to cause a rise in $[Ca^{2+}]_i$ after 24 h pretreatment with 0.1 μM βAsp-8ADT or 1 μM EpoTg (supplemental Fig. S3).

As another potentially significant factor, it has been proposed that Tg-induced cell death in prostate cancer cells requires a supramicromolar rise in $[Ca^{2+}]_i$ (10) mediated by Orai1-dependent SOCE (7). To test whether cell death under our experimental conditions could result from chronic elevated levels of $[Ca^{2+}]_i$, we measured the effect of Tg and the analogs on $[Ca^{2+}]_i$ as a function of incubation time. For this purpose, we chose Fura-2-AM as a $[Ca^{2+}]_i$ indicator because as a ratiometric dye this allows us to accurately compare changes in baseline $[Ca^{2+}]_i$. The measurements were performed on LNCaP and PC3 cells immediately after the addition of inhibitor as well as at several intervals during the first 3 h (Fig. 7, *left panels*). Moreover, cells were, in separate experiments, subjected to daily measurements on freshly loaded samples after 24, 48, and 72 h (Fig. 7, *right panels*). It can be seen from Fig. 7 that over a period of 3 days there is little change in $[Ca^{2+}]_i$ induced by the inhibitors. Notably, the data suggest a tendency of the strong inhibitors to cause a slight *decrease* rather than an increase in $[Ca^{2+}]_i$, especially in the PC3 cells, as would have been expected if there had been a marked influx of Ca^{2+} via any of the Ca^{2+} release-activated channels. Furthermore, to thoroughly test the initial effect of the analogs after addition to Ca^{2+}-filled cells bathed in Ca^{2+}-rich medium, we performed measurements of the effect of Tg and the analogs every 10 min over a period of 3 h after addition of 0.1 μM Tg or O-8–substituted Tg analogs or 1 μM EpoTg. In contrast to previous experiments with exposure of 1 μM O-8–substituted compounds to LNCaP cells (18), we never observed any peak in the initial period after exposure of these inhibitors at 0.1 μM to either PC3 or LNCaP cells (data not shown). This is in line with previous results with 0.1 μM Tg in LNCaP cells (25). In conclusion, in the present experiments, we could not detect any increase in $[Ca^{2+}]_i$ either in acute experiments with measurements performed at 10-min intervals over a period of 0–3 h or by repeated daily measurements over a period of 1–3 days. Thus, it appears that 0.1 μM concentrations of O-8–substituted analogs or 1 μM EpoTg are unable to activate SOCE or other Ca^{2+} influx mechanisms at any measurable

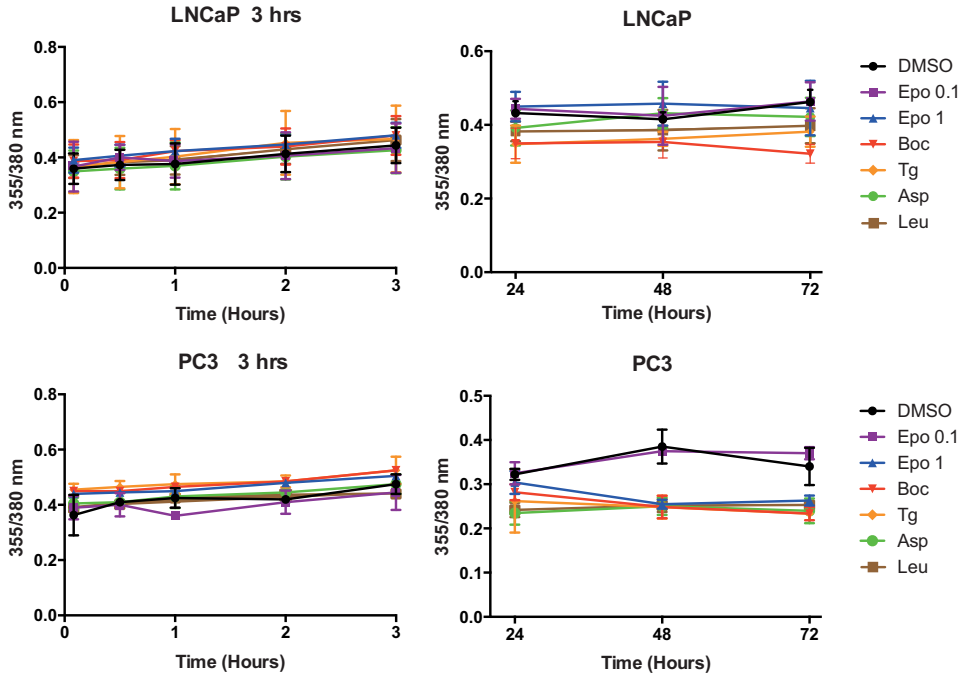

Figure 7. Changes in the cytosolic Ca^{2+} concentration of LNCaP and PC3 cells induced by treatment with Tg and Tg analogs. *Left* and *right panels*, changes in the cytosolic level of Ca^{2+} arising from short-term incubation (0–3 h) (*left panels*) or after 24-, 48-, and 72-h (*right panels*) incubation of cells loaded with Fura-2-AM and exposed to 0.1 μM Tg or O-8–substituted Tg analogs or to 0.1 or 1 μM EpoTg as indicated by changes in the fluorescence emission ratios after alternating excitation of the cells loaded with Fura-2-AM at 355 and 380 nm. The data are means ± S.D. of five experiments with *error bars* representing S.D.

level and therefore that their abilities to induce cell death are unlikely to be caused by bulk increases in the level of free calcium ions in the cytosol.

To complement these findings, we used RNAi to knock down two critical mediators of SOCE, Orai1 and STIM1. As shown in Fig. 8, efficient individual or simultaneous silencing of these two factors did not result in any reduction of Tg-induced cell death in LNCaP, PC3, or MCF7 cells. Similar results were obtained with a second set of siRNAs (data not shown). Thus, SOCE does not appear to contribute to Tg-induced cell death in these experiments.

Cell death induced by Tg and Tg analogs is associated with a strong and sustained UPR—The UPR and in particular the downstream transcription factor CHOP have previously been implicated in Tg-induced cell death (5, 26). To explore the potential role of the UPR under our experimental conditions, LNCaP cells were treated with 0.1 μM Tg or O-8–substituted Tg analogs or 1 μM of EpoTg and immunoblotted for UPR markers at various time points (6, 12, 24, and 48 h). As shown in Fig. 9*A*, treatment with 0.1 μM Tg or 0.1 μM Boc-8ADT (both of which are highly toxic to LNCaP cells; see Fig. 4*A*) resulted in a markedly enhanced expression of ATF4, CHOP, Grp94, and BiP that was maintained for at least 24 h for the former and for at least 48 h for the latter three. ATF4 and CHOP were up-regulated more rapidly than Grp94 and BiP, in line with previous observations in LNCaP cells (25). This sustained UPR observed in response to treatment with 0.1 μM Tg or Boc-8ADT was accompanied by caspase activation as indicated by strongly elevated levels of cleaved PARP at 48 h (Fig. 9*A*). In contrast, treatment with 0.1 μM βAsp-8ADT or 1 μM EpoTg (which are both non-toxic to LNCaP cells; see Fig. 4*A*) had a minor or no effect on the UPR markers and did not induce PARP cleavage (Fig. 9*A*). Treatment with 0.1 μM Leu-8ADT (which induces a low level of cell death in LNCaP cells; see Fig. 4*A*) produced a mild and more transient elevation of ATF4, CHOP, and BiP but no detectable PARP cleavage. In conclusion, caspase activation and severe cell death are associated with a strong and sustained UPR in LNCaP cells. To assess whether the same association could be observed in another cell line, we analyzed UPR activation in PC3 cells treated with a toxic concentrations of Tg or Boc-8ADT (30 nM; see Fig. 4*B*) or with subtoxic concentrations of βAsp-8ADT (10 nM), Leu-8ADT (2 nM), or EpoTg (150 nM). These concentrations of βAsp-8ADT, Leu-8ADT, and EpoTg are all just below or at the lower end of the toxic concentration window (see Fig. 4*B*) and thus would be expected to induce no or little cell death in this experiment. Strikingly, toxic concentrations of Tg and Boc-8ADT strongly enhanced ATF4, CHOP, Grp94, and BiP expression in a manner that was sustained for at least 30 h (Fig. 9*B*), and this was accompanied by a gradual increase in the levels of cleaved PARP (Fig. 9*B*). In contrast, the subtoxic doses of βAsp-8ADT, Leu-8ADT, or EpoTg neither activated the UPR nor induced PARP cleavage (Fig. 9*B*). Microscopy of propidium iodide-probed cells confirmed the absence of appreciable cell death upon treatment of PC3 cells with these concentrations of βAsp-8ADT, Leu-8ADT, or EpoTg for 48 h (Fig. 9*C*), whereas cell death was induced at higher concentrations as expected (Fig. 9*C*). Separate experiments demonstrated sustained UPR induction and PARP cleavage in LNCaP and PC3 cells treated with higher, toxic concentrations of βAsp-8ADT, Leu-8ADT, or EpoTg (data not shown). Taken together, our data indicate the involvement of a

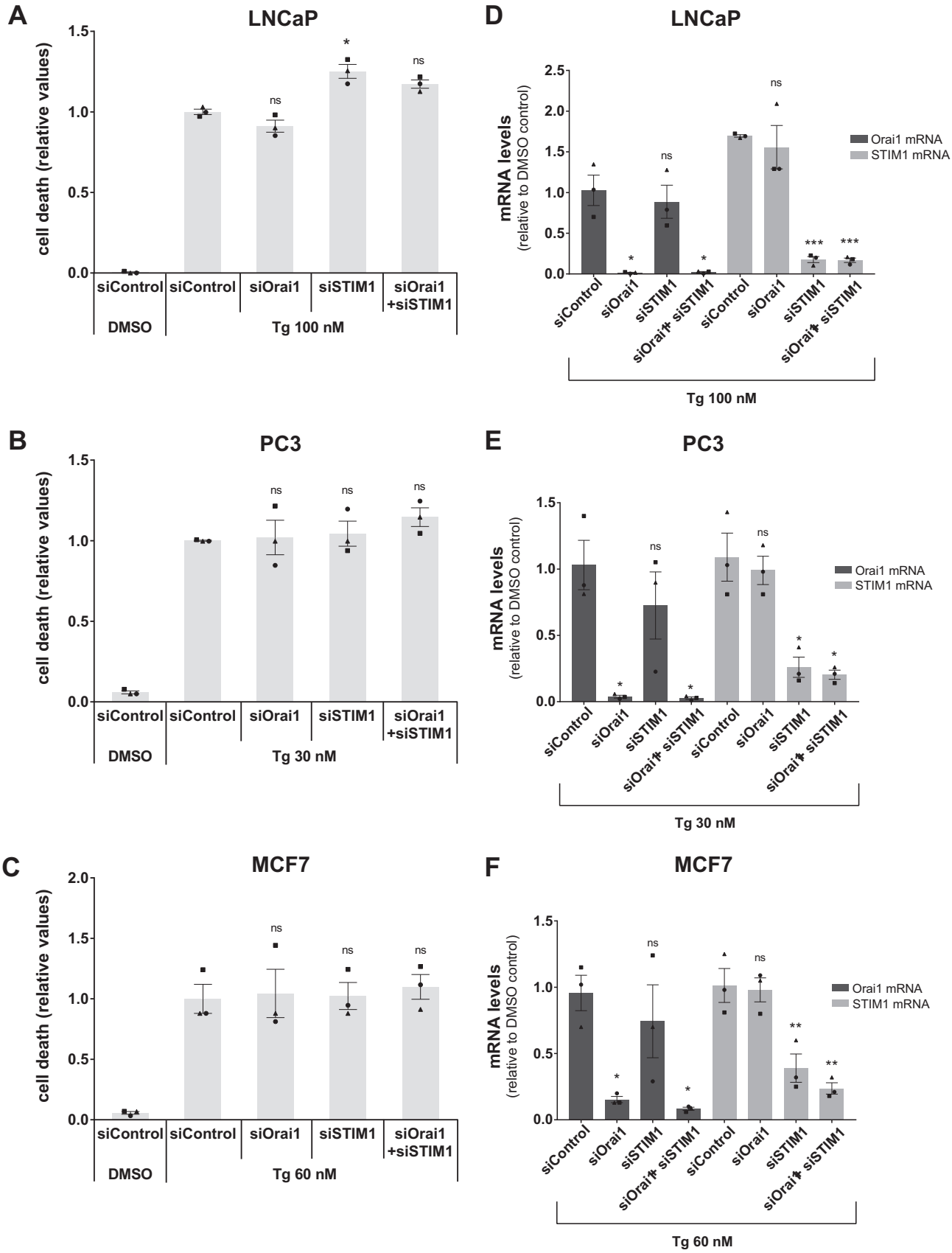
A
LNCaP
cell death (relative values)
siControl
siControl
siOrai1
siSTIM1
siOrai1 +siSTIM1
DMSO
Tg 100 nM
B
PC3
Tg 30 nM
C
MCF7
Tg 60 nM
D
LNCaP
mRNA levels
(relative to DMSO control)
Orai1 mRNA
STIM1 mRNA
Tg 100 nM
E
PC3
Tg 30 nM
F
MCF7
Tg 60 nM

strong and sustained UPR in cell death induced by Tg and Tg analogs in both LNCaP and PC3 cells.

Discussion

Correlations between SERCA inhibition and cellular effects of thapsigargin analogs

Previous biochemical and biophysical studies have identified a high-affinity binding site for Tg at a well-defined intramembranous site of the sarcoplasmic Ca^{2+}-ATPase in the E2 conformational state (27, 28). When binding of Tg occurs to this state, both ATPase activity and Ca^{2+} transport activity are blocked (29–31). The high affinity and specificity with which Tg binds to SERCA have led to the conclusion that the cytotoxic effects of Tg are most likely due to inhibition of SERCA and the disturbances that this provokes with respect to Ca^{2+} homeostasis in the cellular environment. In the present study, we have studied these aspects with a selected number of O-8 side chain-substituted Tg analogs and a derivative of Tg, EpoTg, in which the two geminal hydroxyl groups have been transformed into an epoxy group (Fig. 1*B*). EpoTg was chosen as a model compound because initiating studies had revealed a high affinity for the SERCA pump but poor ability to induce apoptosis. The analogs depicted in Fig. 1, *E* (Leu-8ADT) and *F* (βAsp-8ADT), have been shown to be formed after enzymatic cleavage of, respectively, prodrug G115 by PSA (14) and G202 (mipsagargin) by PSMA (13). Like EpoTg, Boc-8ADT (Fig. 1*D*) also can be regarded as a model compound because it cannot be conjugated with peptide to form a prodrug.

We show that all of the above analogs, whether or not suitable for prodrug synthesis, strongly affect SERCA enzyme activity. Despite that the O-8–substituted analogs only differ in the structure of the N-terminal residue of the O-8 side chain, they do reveal different properties in their effects on cells. This was already noted in a previous publication (18) where it was reported that in particular Boc-8ADT, without measurably affecting $[Ca^{2+}]_i$, had a stronger apoptotic effect on LNCaP cells than the other O-8–substituted analogs. The unchanged cytosolic Ca^{2+} concentration could be accounted for by a slow rate of binding of Boc-8ADT to SERCA, presumably as the result of a hindered penetration of the side chain of the inhibitor between the transmembrane segments of the ATPase (23). However, once the reaction with Boc-8ADT has taken place, SERCA becomes locked into a stable E2–Boc-8ADT complex, and this presumably is the background for the slow release of Ca^{2+} contained within the ER to the cytosol of prostate cells. This contrasts with the effect of Tg where reaction with SERCA gives rise to a rapid efflux of Ca^{2+} from the intracellular Ca^{2+} stores. This efflux is accompanied by a sudden increase of cytosolic Ca^{2+}, an effect that for Tg and the other O-8–substituted analogs is potentiated by uptake of extracellular Ca^{2+} (18), most likely through SOCE mediated by Orai after interaction with the Ca^{2+}-dependent STIM factor localized in the ER (6–8). In the present study, our extended *in vitro* analyses confirm the slow but eventually stable mode of action of Boc-8ADT with SERCA. Importantly, with the *in vivo* analyses in three different cell lines (LNCaP, PC3, and MCF7), we can now demonstrate that Boc-8ADT, despite the slow mode of interaction with SERCA, shows better toxicity than all the other Tg analogs in all three cell lines. Thus, we conclude that rapid depletion of ER Ca^{2+} accompanied by a rapid rise of $[Ca^{2+}]_i$, as observed with Tg, is not required for cell death induced by SERCA inhibition.

In the present study, we found that in particular EpoTg had notable and different properties on SERCA function and Ca^{2+} homeostasis than the other Tg analogs. Although EpoTg is commercially advertised as an inactive Tg analog, our current detailed investigations revealed that EpoTg is in fact a Ca^{2+} pump inhibitor with high affinity for SERCA. Nevertheless and in contrast to the other analogs, EpoTg allows some ATPase activity to occur even in the presence of high inhibitor concentrations, and this effect was combined with the ability to sustain an appreciable degree of Ca^{2+} accumulation in isolated, tight longitudinal sarcoplasmic reticulum (SR) vesicles. The active transport of Ca^{2+} observed under these conditions can be attributed to simultaneous interaction of SERCA with EpoTg and Ca^{2+}, leading to the formation of hybrid complexes such as Ca_2E1–EpoTg. The equilibrium level of Ca^{2+} accumulated inside the SR vesicles was much less affected than would be predicted from the observed decrease in ATP hydrolysis and initial Ca^{2+} transport rates. However, assays on isolated tight SR vesicles cannot be directly compared with activity assays (32, 33). This is mainly a consequence of the high intravesicular accumulation of Ca^{2+}, which in addition to decreasing ATPase activity also activates a Ca^{2+}/Ca^{2+} exchange mechanism coupled to the ATPase-supported Ca^{2+} uptake (32, 33), probably as a substitute of the Ca^{2+}/H^+ exchange taking place at low intra-/extravesicular Ca^{2+} ratios (34). Despite the inhibition of ATPase function by the EpoTg-doped vesicles, these factors tend to maintain vesicular Ca^{2+} accumulation at a constant and maximal level even in the face of the large reductions of ATPase activity observed at high intravesicular Ca^{2+} concentrations.

Figure 8. SOCE is not required for Tg-induced cell death. *A–C*, LNCaP (*A*), PC3 (*B*), or MCF7 (*C*) cells were seeded in 96-well plates, reverse transfected with 10 nM non-targeting control siRNA ("siControl") or siRNAs targeting Orai1 (si*Orai1*) or STIM1 (si*STIM1*), and incubated for 2 days. Subsequently, the cells were treated with DMSO vehicle control (0.1%) or the indicated concentrations of Tg together with 2.5 μg/ml propidium iodide in complete medium. Cell death was assessed using an Incucyte instrument for automated live-cell imaging and calculation of red fluorescence and total cell confluence. Cell death is plotted as the ratio of red fluorescence to total cell confluence after 48 h, normalized to that obtained with Tg in siControl-transfected cells. Data are means ± S.E. from three independent experiments. Single symbols represent individual measurements for each cell line (each symbol represents the mean value from triplicate wells), and each experiment is indicated by differently shaped symbols. *, $p < 0.05$; *ns*, not significant (*i.e.* $p \geq 0.05$), paired Student's *t* test compared with Tg/siControl. *D–F*, in parallel with the transfection in *A–C*, LNCaP (*D*), PC3 (*E*), or MCF7 (*F*) cells were transfected with the same RNAi mixture in 6-well plates. After 2 days of transfection and 48 h of treatment with Tg, the cells were harvested and extracted for RNA to confirm the knockdown of Orai1 and STIM1. The mRNA levels were assessed by real-time RT-PCR. Relative levels normalized to that found with DMSO in siControl-transfected cells are shown. Data are means ± S.E. from three independent experiments with *error bars* representing S.E. Single symbols represent individual values for each cell line (each symbol represents the mean value from triplicate measurements), and each experiment is indicated by differently shaped symbols. *, $p < 0.05$; **, $p < 0.01$; ***, $p < 0.001$; *ns*, not significant (*i.e.* $p \geq 0.05$), paired Student's *t* test compared with Tg/siControl.

In contrast, Tg and the O-8–substituted analogs behave as straightforward inhibitors of SERCA function: they efficiently inhibited Ca^{2+} transport, ATP hydrolysis, and Ca^{2+} binding when bound to SERCA. This inhibition is not irreversible as it is often stated to be for Tg, but it requires dissociation of the inhibitors from the firmly bound E2 complexes of SERCA, *e.g.* by gel chromatography, by dilution with large volumes of inhibitor-free medium, or more rapidly by addition of high (millimolar) concentrations of Ca^{2+}. This induces a conformational change of SERCA to the Ca_2E1-ATP state and thereby displaces Tg or O-8–substituted analogs from SERCA.

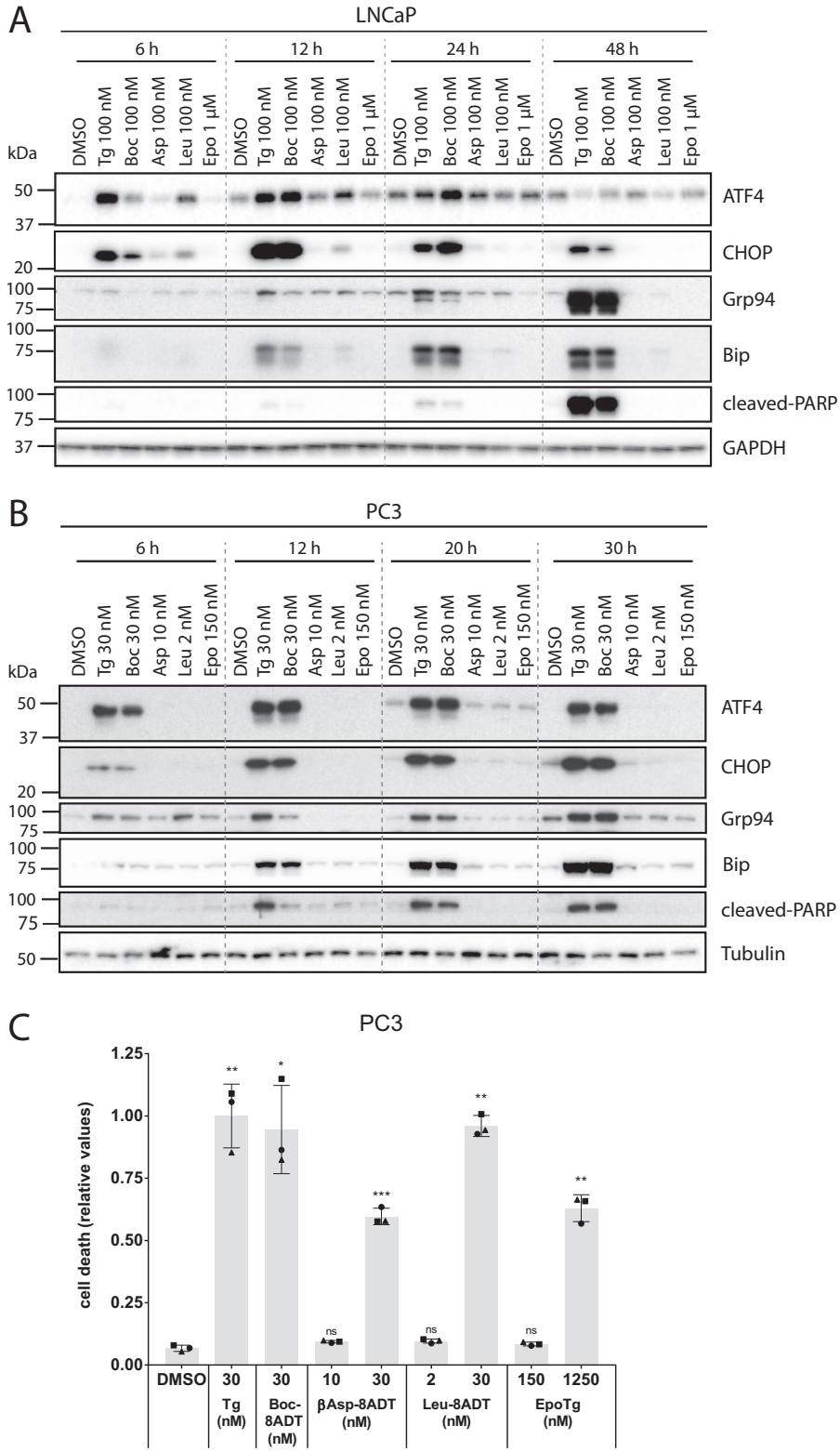

The role of cytosolic Ca^{2+} and SOCE in cell death induced by Tg and Tg analogs

According to previous investigations, the immediate effects of Tg on $[Ca^{2+}]_i$ subside after a number of hours followed by a subsequent rise that results in supramicromolar $[Ca^{2+}]_i$ levels (10, 11). To account for the harmful long-term effects of Tg, it has been proposed that this substantial increase in $[Ca^{2+}]_i$ causes calmodulin, calpain, and calcineurin to trigger a number of intracellular phosphorylation and cleavage reactions that lead to apoptotic cell death (10–12). However, this view has been challenged by reports that indicate a suppressive role of calcineurin and calpains on caspase activation and cell death (35–38). Importantly, our data strongly suggest that cell death induced by Tg and O-8–substituted Tg analogs does not require the previously implied increased levels of $[Ca^{2+}]_i$. The first clue came from our observations made here and previously (18) that Boc-8ADT does not inflict any tangible effect on $[Ca^{2+}]_i$ in any of the cell lines tested. This is probably due to the slow kinetics with which this analog reacts with SERCA and the correspondingly slow net leakage of Ca^{2+} from the ER, which likely allows sufficient time for continuous maintenance of a constant $[Ca^{2+}]_i$ via compensatory homeostatic mechanisms. The lack of any tangible effect on $[Ca^{2+}]_i$ by Boc-8ADT contrasts with the deleterious effects that this Tg analog exerts in long-term experiments in LNCaP cells (Ref. 18 and this study) as well as in PC3 and MCF7 cells (this study). Emphasizing the importance of these observations, we now find that the deviant behavior of Boc-8ADT can be extended to Tg and other analogs modified at the O-8 side chain when the inhibitor concentration is reduced to 0.1 μM instead of 1 μM used previously (18). Under these conditions, $[Ca^{2+}]_i$ was not increased, indicating absence of SOCE activation, in the three cell lines tested. Thus, with analogy to the previous Boc-8ADT experiments with LNCaP cells, the maintenance of a low $[Ca^{2+}]_i$ in PC3 and MCF7 cells did not prevent the cells from undergoing apoptosis in long-term experiments (3–6 days) where exposure to 0.1 μM inhibitor was as efficient to induce cell death as exposure of the cells to 1 μM inhibitor. Therefore, these data obtained on cells with a depleted ER Ca^{2+} content do not support cytosolic Ca^{2+} cytotoxicity as being involved in the apoptotic response reported here. In support of this conclusion and further discarding a role for the SOCE process in Tg-induced apoptosis, our RNAi experiments showed that efficient, simultaneous silencing of the critical SOCE mediators Orai1 and STIM1 did not have any protective effect in LNCaP, PC3 or MCF7 cells. As a cautionary note, our results do not necessarily rule out that Ca^{2+} cytotoxicity could be involved as an important factor under other circumstances. For example, in a previous study, it was shown that, although Tg-induced death of renal cells was unaffected by calpain inhibition, calpains were important for cell death induced by reactive chemical toxicants (39). Moreover, our findings do not exclude the possibility that the cell membranes in general become leaky before apoptotic cell death occurs, and such a change will ultimately lead to an unspecific increase in cell permeability for Ca^{2+}. Lastly, because apoptosis in cell populations is an asynchronous process, it is possible that in the final steps of cell death there could be an appreciable, asynchronous increase in $[Ca^{2+}]_i$ at the single-cell level that is too brief to be appreciated when observing a large cell population.

ER Ca^{2+} depletion and UPR as a transition state to cell death

Collectively, our experiments with Tg and different Tg analogs demonstrate an association between long-term depletion of ER Ca^{2+} (as measured after 24 h of treatment) and subsequent cell death. Our use of Tg analogs with different SERCA interaction properties reveals some very interesting aspects with regard to this relationship. First, because 0.1 μM Boc-8ADT showed high cytotoxic potency despite inducing a very slow release of ER Ca^{2+}, the rate of ER Ca^{2+} depletion is clearly not a decisive factor for cell death. Second, our experiments using 1 μM EpoTg in PC3 cells suggest that persistent but incomplete inhibition of SERCA (our *in vitro* experiments demonstrated that even very high concentrations of EpoTg did not fully inhibit SERCA) is sufficient to induce ER Ca^{2+} depletion and cell death. In fact, even 0.1 μM EpoTg, which would be expected to show only a mild inhibitory effect on SERCA Ca^{2+} transport, was able to partially deplete the ER of Ca^{2+}. However, such a partial depletion was not sufficient to induce cell death. Moreover, it was not sufficient to activate the UPR as assessed by expression analyses of downstream UPR components. Indeed, our further analysis demonstrated that caspase activation and cell death occur solely under conditions where Tg or Tg analogs are able to mount a strong and sustained UPR. Taken together, we conclude that the major determinants of cell death induced by Tg and Tg analogs are likely to be long-term ER Ca^{2+} depletion and a sustained UPR, whereas SOCE and high cytosolic Ca^{2+} levels do not appear to be required. Future studies will be aimed at determining what degree of ER Ca^{2+} depletion is required for a cell death-inducing UPR. Moreover, it will be important to decipher the roles of the var-

Figure 9. Only toxic concentrations of Tg and Tg analogs induce a sustained UPR. LNCaP (*A*) or PC3 (*B*) cells were seeded in 6-well plates and grown for 2 days upon which they were treated for four different time points (as indicated) with toxic concentrations of Tg or Boc-8ADT (100 nM in LNCaP and 30 nM in PC3) or with low/subtoxic concentrations of βAsp-8ADT (100 nM in LNCaP and 10 nM in PC3), Leu-8ADT (100 nM in LNCaP and 2 nM in PC3), or EpoTg (1 μM in LNCaP and 150 nM in PC3). Protein lysates were prepared and analyzed by immunoblotting to assess the expression levels of the indicated proteins (ATF4, CHOP, Grp94, and BiP as UPR indicators and cleaved PARP as a marker for caspase activity). GAPDH and tubulin were used as loading controls. The *dotted lines* are inserted for visual aid only (*i.e.* the membranes were not spliced). One representative experiment of three independent experiments is shown for each cell line. The positions of molecular mass markers are indicated to the *left* of the blots. *C*, PC3 cells were seeded in 96-well plates and incubated for 2 days. Subsequently, the cells were treated with DMSO control or the indicated concentrations of Tg, Boc-8ADT, βAsp-8ADT, Leu-8ADT, or EpoTg together with 2.5 μg/ml propidium iodide in complete medium. Cell death was assessed using an Incucyte instrument for automated live-cell imaging and calculation of red fluorescence and total cell confluence. Cell death is plotted as the ratio of red fluorescence to total cell confluence after 48 h, normalized to that obtained with Tg. Data are means ± S.E. from three independent experiments with *error bars* representing S.E. Single symbols represent individual measurements (each symbol represents the mean value from triplicate wells), and each experiment is indicated by differently shaped symbols. *, $p < 0.05$; **, $p < 0.01$; ***, $p < 0.001$; *ns*, not significant (*i.e.* $p \geq 0.05$), paired Student's *t* test compared with DMSO control.

ious UPR arms and downstream factors in Tg-induced cell death.

Efficiency of the analogs as antineoplastic agents

Our data demonstrate a solid overall correlation between SERCA inhibition and cell death: Tg and Boc-8ADT are the most efficient compounds in both respects, but Leu-8ADT is also fully capable of both inhibiting SERCA and provoking cell death. However, our data give little clues as to why βAsp-8ADT, which also has a high inhibitory potency against SERCA, stands apart in comparison with other O-8–modified analogs as a weaker inducer of cell death and a weaker antiproliferative agent. Our Ca^{2+} dissociation experiments indicated a slower release of the second calcium ion from SERCA by βAsp-8ADT than was observed with Leu-8ADT, suggesting a different mode of interaction of βAsp-8ADT with SERCA. It is tempting to speculate that this could be relevant for the differential cellular effects. However, this speculation simultaneously reveals a knowledge gap in understanding how subtle differences in SERCA modulation can alter resulting cellular effects. Clearly, the question why βAsp-8ADT acts differently in cells than other O-8–substituted Tg analogs warrants further study, especially in relation to clinical trials showing promising effects of a polyglutamic prodrug of βAsp-8ADT (G202; mipsagargin) in patients suffering from hepatocellular carcinoma and glioblastoma multiforme (17). Interestingly, apart from having cell death-inducing and antiproliferative effects, Tg has also been shown to potently inhibit the lysosomal degradative pathway autophagy in cancer cells, including in LNCaP cells at a Tg concentration of 0.1 μM (25). In light of the emerging clinically relevant role of the autophagic process in cancer and many other diseases (40), it will in future studies be of interest to determine and compare the effects of βAsp-8ADT and other Tg analogs on autophagy. This may provide for a deeper understanding of how SERCA inhibition affects cellular processes related to cell fate, as well as how this can be exploited in therapeutic settings.

Experimental procedures

Materials

Cell experiments were conducted with LNCaP and PC3 prostate cancer cells obtained from ATCC and grown in RPMI 1640 supplemented with 5 mM L-glutamine, 10% fetal bovine serum (FBS), 100,000 IU/liter penicillin, and 100 mg/liter streptomycin. MCF7 breast cancer cells (ATCC) were grown in Dulbecco's modified eagle medium (DMEM) with 10% FBS and penicillin/streptomycin as for the prostate cells. Thapsigargin (Fig. 1*A*) was supplied by Alomone Labs (Jerusalem, Israel) or Sigma-Aldrich, whereas EpoTg (Fig. 1*B*) (41) and the analogs of thapsigargin with O-8–aminododecanoyl linkers shown in Fig. 1, *C–F*, were prepared as described previously (42). Stock solutions of these compounds dissolved in dimethyl sulfoxide (DMSO) were stored at −20 °C in HEPES-buffered saline (HBS), which consisted of 138 mM Na^+, 132.9 mM Cl^-, 5.3 mM K^+, 1.8 mM Ca^{2+}, 0.8 mM Mg^{2+}, 0.8 mM SO_4^{2-}, 5.6 mM glucose, and 14 mM HEPES (pH 7.4 at 37 °C). SERCA1a membranes were prepared from sarcoplasmic reticulum vesicles of rabbit skeletal muscle and purified by extraction with a low concentration of deoxycholate to remove extrinsic proteins according to established procedures (43).

Properties of the thapsigargin analogs selected for investigation

In terms of chemical structure, Tg is a guaianolide with a three-ring structure formed by annulation of a cycloheptane, a cyclopentene, and a γ-lactone (Fig. 1*A*). The rings are highly oxygenated with hydroxyl groups esterified by octanoic acid at O-2, by angelic acid at O-3, by butanoic acid at O-8, by acetate at O-10, and with unreacted hydroxyl groups at C-7 and C-11. The ester bond at O-8 is of particular interest for preparation of prodrugs because it can easily be subjected to hydrolysis, leading to debutanoyl-Tg. This product can be used to introduce almost any carboxylic acid at O-8. With this in mind, we have explored the properties of a variety of Tg analogs where the butanoyl side chain at O-8 has been replaced by 12-aminododecanoate to form 8ADT (Fig. 1*C*) and further modified N-terminally by Boc to form Boc-8ADT (Fig. 1*D*) or by different amino acid residues to form Leu-8ADT (Fig. 1*E*) and βAsp-8ADT (Fig. 1*F*). Among these, Leu-8ADT (Fig. 1*E*) and βAsp-8ADT (Fig. 1*F*) represent the active components of drugs designed to kill prostate cancer and endothelial cells in neovascular tumor tissue (13, 14) following cleavage of the prodrugs G115 and G202 by PSA and PSMA, respectively (see the Introduction). Furthermore, of importance for our analysis of the biological effect of the analogs, our investigation also included a Tg analog of another type, EpoTg, the epoxide of Tg where C-7 and C-11 are joined by a β-oxygen bridge (Fig. 1*B*).

Effects of thapsigargin and analogs on cell survival and function

To follow the long-term cellular effects of Tg and the analogs, cells were seeded in 24-well plates (Nunc) at around 5000 cells/well and incubated overnight under standard conditions at 37 °C and 5% CO_2 prior to exposure to Tg and Tg analogs. The effects on morphology and live cell counts (densities) were then followed over 1–6 days by phase-contrast microscopy with daily counting of surviving (non-apoptotic and non-necrotic) cells remaining as a function of time in a predefined, representative field close to the center of the wells. For automated live-cell imaging, cells were seeded in clear 96-well plates (Falcon) for 2–3 days prior to treatment and placed in an Incucyte ZOOM instrument located inside a normal, humidified cell incubator containing 5% CO_2. To measure cell death, 2.5 μg/ml propidium iodide (Merck/Calbiochem) was added simultaneously with the treatments, which were done in triplicate wells in each experiment (*i.e.* three replicate wells per treatment condition). Multiple pictures from each well were taken every 3 h. For analysis, cell masks were set using the Incucyte ZOOM software and following the recommendations from the provider. The software algorithm was used to calculate cell confluence for each time point (provided as percent cell density), which subsequently was normalized for representation as -fold change compared with time 0. Cell death was expressed as the ratio of red fluorescence to total cell confluence. $LD_{50(Tg\text{-}max)}$ values (defined as the Tg or Tg analog concentration required to obtain 50% of the maximal Tg response) were calculated

using GraphPad Prism7 to generate and analyze sigmoid semilogarithmic plots of data points from four (LNCaP and MCF7) or five (PC3) independent experiments.

Intracellular Ca^{2+} measurements

$[Ca^{2+}]_i$ measurements were performed on a Mithras LB940 microplate reader instrument (Berthold Technologies). PC3 cells (75,000/well) and LNCaP cells (50,00/well) were seeded on black, clear bottomed poly-D-lysine-coated 96-well microplates and grown to confluence for 1–2 days. Before an experiment, the cells were loaded for 30 min at 37 °C with 5 μM Fluo-4-AM (Life technologies) dissolved in Ca^{2+}-containing HBS (pH 7.4) with the composition described above. The fluorophore was then removed by rinsing with HBS followed by thermoequilibration at room temperature for 20 min. At the start of the experiment, the buffer was replaced with a nominally Ca^{2+}-free HBS containing 1 mM EGTA. Recordings were started with baseline measurements (12 observations at 0.5 Hz) of the fluorophore fluorescence excited at 488 nm and recorded at 535 nm. After 10 min, 1 μM Tg or the analogs was added with a multipipette, and the experiments were continued for up to 35 min to register the effect of the inhibitors on the release of Ca^{2+} from the Tg-sensitive ER stores to the cytosol. To measure the effect of pretreatment with SERCA pump inhibitors, preseeded cells were in other experiments first incubated for 24 h with a 0.1 or 1 μM concentration of Tg or Tg analogs prior to loading with 5 μM Fluo-4-AM. After rinsing the cells for 10 min with EGTA-containing but inhibitor-free HBS, we then tested whether it was possible to elicit a rise in $[Ca^{2+}]_i$ by addition of 1 μM Tg. When the addition of Tg resulted in a $[Ca^{2+}]_i$ increase, this was taken as an indication that the emptying of Ca^{2+} from the ER had been incomplete during the preceding 24-h preincubation. The effect of analog preincubation was estimated by comparison with the effect observed by addition of 1 μM Tg to DMSO control cells, which had not been pretreated with inhibitor and thus could be considered to have maintained an intact ER Ca^{2+} content.

To study the long-term effects of the SERCA pump inhibitors on $[Ca^{2+}]_i$, we followed by 10 repetitive scans the changes in baseline $[Ca^{2+}]_i$ in both acute (0–3-h) experiments and by daily measurements over a period of the following 3 days. For this purpose, the cell samples were measured immediately after loading of the cells with Fura-2-AM in HBS, and signals were obtained after excitation at 355 and 380 nm with collection of emission at 515 nm. In these experiments, $[Ca^{2+}]_i$ was expressed as a ratio of the emitted light after alternating excitation at 355/380 nm where 355 nm is close to the isosbestic point for Fura-2 and thus independent of the Ca^{2+} concentration. The 355/380 nm ratio was chosen rather than 340/380 nm because of the severe loss of 340 nm light through regular glass as used in the black 96-well plates.

Enzyme activity

The effect of the Tg analogs on the ATPase activity of purified SERCA preparations was measured by enzymatic spectrophotometry from the decrease in absorption at 340 nm with an ATP- and NADH-coupled system according to a protocol described previously (23). Purified SERCA pump membranes (1 mg of protein/ml), suspended in a buffer containing 10 mM TES (pH 7.5), 100 mM KCl, 1 mM $MgCl_2$, and 1 mM EGTA, were added sequentially in 10-μl aliquots to a 23 ± 0.2 °C thermostated cuvette compartment containing 3 ml of the same buffer without EGTA but supplemented with 0.1 mM Ca^{2+}, 1 mM phosphoenolpyruvate, 0.175 mM NADH, 65 units of phosphoenolpyruvate kinase, and 82 units of lactate dehydrogenase. Unless otherwise noted (as for Boc-8ADT; Fig. 2*C*) activity was measured by addition of 5 mM ATP 3–6 min after each addition of inhibitor to the ATPase suspension to allow sufficient time for the inhibitors to interact fully with the ATPase before the activity measurement.

Time-resolved Ca^{2+} dissociation

The effect of time on the dissociation of Ca^{2+} from the inhibitor-treated ATPase membranes in the Ca_2E1 conformation was measured with radiolabeled $^{45}Ca^{2+}$ and Millipore filtration as described previously (23). Tg and Tg analogs were added at a high concentration (12 μM) to Ca^{2+}-ATPase (0.1 mg protein/ml; *i.e.* <1 μM) suspended in 50 μM $^{45}Ca^{2+}$, 50 mM MOPS (pH 7.2), 100 mM KCl, and 5 mM Mg^{2+}. At timed intervals, 2-ml aliquots were passed without rinsing through a double layer of Millipore HA filters (size, 0.45 μm). After radioactive counting, the Ca^{2+} bound to the ATPase was calculated by subtracting the counts in the lower, protein-free filters from the counts on the upper filters with deposited Ca^{2+}-ATPase.

$^{45}Ca^{2+}$ transport

The effect of EpoTg and other Tg analogs on Ca^{2+} transport was studied with $^{45}Ca^{2+}$ and Millipore filtration on tight SR vesicle preparations. In these experiments, 1–10 μM inhibitor was preincubated for 5 or 1440 min with 0.05 mg/ml SR suspended in 50 mM MOPS (pH 7.2), 100 mM KCl, 5 mM $MgCl_2$, and 0.1 mM EGTA. The Ca^{2+} transport reaction was started by addition of 0.08 mM MgATP, 0.02 mM $^{45}Ca^{2+}$, and inhibitor-free samples (resulting in a calculated concentration of free Ca^{2+} of 1 μM in the presence of EGTA to approximate cytosolic conditions). Immediately after addition of MgATP, 0.2-ml aliquots of reaction mixture were taken at different time intervals (from 10 s up to 15 min) and quenched with 4 ml of ice-cold buffer. The sample was Millipore filtered and rinsed twice with 3 ml of ice-cold buffer before counting of radioactivity.

siRNA transfections

LNCaP, PC3, and MCF7 cells were reverse transfected with siRNA using Opti-MEM reduced serum medium (Gibco 11058) and Lipofectamine RNAiMax (Invitrogen 13778) as described previously (25) except that the transfection was additionally scaled down to 96-well format (for cell death measurements) and to a final siRNA concentration of 10 nM. Experiments were initiated 2 days after transfection. The following siRNAs were used (all Silencer® Select siRNAs from Ambion): Silencer Select Negative Control Number 1 (4390843), si*Orai1* (s39560), and si*STIM1* (s13562). Additionally, a second set of siRNAs were used that gave very similar results: si*Orai1* (s228396) and si*STIM1* (s13561).

Real-time RT-PCR

Cells were harvested and washed in cold PBS and 0.5% FBS before total RNA extraction using the IllustraRNAspin Mini isolation kit (GE Healthcare 25-0500-71). Total RNA was reverse transcribed using SuperScript VILO Master Mix (Applied Biosystems 11755250). Quantitative real-time RT-PCR was performed using TaqMan gene expression assays (Applied Biosystems) with TaqMan Fast Advanced PCR Master Mix (Applied Biosystems 4444558). PCR amplification was done in triplicate series with the ABI 7900HT FAST sequence detection system (Applied Biosystems). The cycling conditions were 50 °C for 2 min, 95 °C for 10 min, 40 cycles at 95 °C for 15 s, and 60 °C for 1 min. Relative transcript levels were determined by the comparative C_T method and normalization to the mean C_T value of TBP. The following TaqMan gene expression assay probes (Applied Biosystems) were used: Orai1 (Hs03046013_m1), STIM1 (Hs00963373_m1), and TBP (Hs99999910_m1).

SDS-PAGE and immunoblot analysis

Preparation of whole-cell lysates, SDS-PAGE, and immunoblot analysis were performed as described previously (25). Primary antibodies against the following proteins were used:α-tubulin (Abcam ab7291), ATF4 (Cell Signaling Technology 11815), BiP (Cell Signaling Technology 3177), CHOP (Cell Signaling Technology 211195), cleaved PARP (Cell Signaling Technology 5625), GAPDH (Cell Signaling Technology 2118), and Grp94 (Cell Signaling Technology 2104). Secondary horseradish peroxidase-conjugated goat anti-rabbit (Dako) and rabbit anti-mouse (Dako) antibodies were used at 1:5000 dilutions.

Author contributions—J. V. M., S. B. C., and N. E. were in charge of the experiments. P. Sehgal, P. Szalai, C. O., H. A. P., P. N., S. B. C., N. E., and J. V. M. designed the experiments, which were performed and analyzed by P. Sehgal, P. Szalai, and C. O. The manuscript was written by J. V. M. together with N. E. and with inputs from all authors.

Acknowledgments—We are grateful to Prof. David W. Andrews and Jarkko Ylanko for assistance to postdoctoral fellow Pankaj Sehgal, the use of the laboratory to perform many of the cell biological experiments, and inspiring discussions on all aspects of the present work. We give special thanks to Huizhen Lui at S. B. Christensen's laboratory for contributing to the synthesis of the Tg analogs. We also thank Lisbeth Nielsen, Birte Nielsen, Anne Lillevang, and Frank Sætre for competent technical assistance and express thanks to Dr. Steffen Junker (Department of Biomedicine, Aarhus University) for expert guidance with the cytological experiments at Aarhus University.

References

1. Carafoli, E. (2002) Calcium signaling: a tale for all seasons. *Proc. Natl. Acad. Sci. U.S.A.* **99,** 1115–1122
2. Schwarze, S. R., Lin, E. W., Christian, P. A., Gayheart, D. T., and Kyprianou, N. (2008) Intracellular death platform steps-in: targeting prostate tumors via endoplasmic reticulum (ER) apoptosis. *Prostate* **68,** 1615–1623
3. Wang, M., and Kaufman, R. J. (2014) The impact of the endoplasmic reticulum protein-folding environment on cancer development. *Nat. Rev. Cancer* **14,** 581–597
4. Lee, J., and Ozcan, U. (2014) Unfolded protein response signaling and metabolic diseases. *J. Biol. Chem.* **289,** 1203–1211
5. Lu, M., Lawrence, D. A., Marsters, S., Acosta-Alvear, D., Kimmig, P., Mendez, A. S., Paton, A. W., Paton, J. C., Walter, P., and Ashkenazi, A. (2014) Opposing unfolded-protein-response signals converge on death receptor 5 to control apoptosis. *Science* **345,** 98–101
6. Deng, X., Wang, Y., Zhou, Y., Soboloff, J., and Gill, D. L. (2009) STIM and Orai: dynamic intermembrane coupling to control cellular calcium signals. *J. Biol. Chem.* **284,** 22501–22505
7. Flourakis, M., Lehen'kyi, V., Beck, B., Raphaël, M., Vandenberghe, M., Abeele, F. V., Roudbaraki, M., Lepage, G., Mauroy, B., Romanin, C., Shuba, Y., Skryma, R., and Prevarskaya, N. (2010) Orai1 contributes to the establishment of an apoptosis-resistant phenotype in prostate cancer cells. *Cell Death Dis.* **1,** e75
8. Parekh, A. B., and Putney, J. W. (2005) Store-operated calcium channels. *Physiol. Rev.* **85,** 757–810
9. Orrenius, S., Zhivotovsky, B., and Nicotera, P. (2003) Regulation of cell death: the calcium-apoptosis link. *Nat. Rev. Mol. Cell Biol.* **4,** 552–565
10. Tombal, B., Weeraratna, A. T., Denmeade, S. R., and Isaacs, J. T. (2000) Thapsigargin induces a calmodulin/calcineurin-dependent apoptotic cascade responsible for the death of prostatic cancer cells. *Prostate* **43,** 303–317
11. Vander Griend, D. J., Antony, L., Dalrymple, S. L., Xu, Y., Christensen, S. B., Denmeade, S. R., and Isaacs, J. T. (2009) Amino acid containing thapsigargin analogues deplete androgen receptor protein via synthesis inhibition and induce the death of prostate cancer cells. *Mol. Cancer Ther.* **8,** 1340–1349
12. Denmeade, S. R., and Isaacs, J. T. (2005) The SERCA pump as a therapeutic target: making a "smart bomb" for prostate cancer. *Cancer Biol. Ther.* **4,** 14–22
13. Denmeade, S. R., Mhaka, A. M., Rosen, D. M., Brennen, W. N., Dalrymple, S., Dach, I., Olesen, C., Gurel, B., Demarzo, A. M., Wilding, G., Carducci, M. A., Dionne, C. A., Møller, J. V., Nissen, P., Christensen, S. B., *et al.* (2012) Engineering a prostate-specific membrane antigen-activated tumor endothelial cell prodrug for cancer therapy. *Sci. Transl. Med.* **4,** 140ra86
14. Denmeade, S. R., Jakobsen, C. M., Janssen, S., Khan, S. R., Garrett, E. S., Lilja, H., Christensen, S. B., and Isaacs, J. T. (2003) Prostate-specific antigen-activated thapsigargin prodrug as targeted therapy for prostate cancer. *J. Natl. Cancer Inst.* **95,** 990–1000
15. Levy, O., Brennen, W. N., Han, E., Rosen, D. M., Musabeyezu, J., Safaee, H., Ranganath, S., Ngai, J., Heinelt, M., Milton, Y., Wang, H., Bhagchandani, S. H., Joshi, N., Bhowmick, N., Denmeade, S. R., *et al.* (2016) A prodrug-doped cellular Trojan horse for the potential treatment of prostate cancer. *Biomaterials* **91,** 140–150
16. Denmeade, S. R., Lou, W., Lövgren, J., Malm, J., Lilja, H., and Isaacs, J. T. (1997) Specific and efficient peptide substrates for assaying the proteolytic activity of prostate-specific antigen. *Cancer Res.* **57,** 4924–4930
17. Mahalingam, D., Wilding, G., Denmeade, S., Sarantopoulas, J., Cosgrove, D., Cetnar, J., Azad, N., Bruce, J., Kurman, M., Allgood, V. E., and Carducci, M. (2016) Mipsagargin, a novel thapsigargin-based PSMA-activated prodrug: results of a first-in-man phase I clinical trial in patients with refractory, advanced or metastatic solid tumours. *Br. J. Cancer* **114,** 986–994
18. Dubois, C., Vanden Abeele, F., Sehgal, P., Olesen, C., Junker, S., Christensen, S. B., Prevarskaya, N., and Møller, J. V. (2013) Differential effects of thapsigargin analogues on apoptosis of prostate cancer cells: complex regulation by intracellular calcium. *FEBS J.* **280,** 5430–5440
19. Søhoel, H., Jensen, A.-M., Møller, J. V., Nissen, P., Denmeade, S. R., Isaacs, J. T., Olsen, C. E., and Christensen, S. B. (2006) Natural products as starting materials for development of second-generation SERCA inhibitors targeted towards prostate cancer cells. *Bioorg. Med. Chem.* **14,** 2810–2815
20. Toyoshima, C., Nakasako, M., Nomura, H., and Ogawa, H. (2000) Crystal structure of the calcium pump of sarcoplasmic reticulum at 2.6 Å resolution. *Nature* **405,** 647–655
21. Lee, A. G., and East, J. M. (2001) What the structure of a calcium pump tells us about its mechanism. *Biochem. J.* **356,** 665–683
22. Musgaard, M., Thøgersen, L., Schiøtt, B., and Tajkhorshid, E. (2012) Tracing cytoplasmic Ca^{2+} ion and water access points in the Ca^{2+}-ATPase. *Biophys. J.* **102,** 268–277

23. Winther, A.-M., Liu, H., Sonntag, Y., Olesen, C., le Maire, M., Soehoel, H., Olsen, C.-E., Christensen, S. B., Nissen, P., and Møller, J. V. (2010) Critical roles of hydrophobicity and orientation of side chains for inactivation of sarcoplasmic reticulum Ca^{2+}-ATPase with thapsigargin and thapsigargin analogues. *J. Biol. Chem.* **285,** 28883–28892
24. Papp, B., Brouland, J.-P., Arbabian, A., Gélébart, P., Kovács, T., Bobe, R., Enouf, J., Varin-Blank, N., and Apáti, A. (2012) Endoplasmic reticulum calcium pumps and cancer cell differentiation. *Biomolecules* **2,** 165–186
25. Engedal, N., Torgersen, M. L., Guldvik, I. J., Barfeld, S. J., Bakula, D., Sætre, F., Hagen, L. K., Patterson, J. B., Proikas-Cezanne, T., Seglen, P. O., Simonsen, A., and Mills, I. G. (2013) Modulation of intracellular calcium homeostasis blocks autophagosome formation. *Autophagy* **9,** 1475–1490
26. Yamaguchi, H., and Wang, H.-G. (2004) CHOP is involved in endoplasmic reticulum stress-induced apoptosis by enhancing DR5 expression in human carcinoma cells. *J. Biol. Chem.* **279,** 45495–45502
27. Toyoshima, C., and Nomura, H. (2002) Structural changes in the calcium pump accompanying the dissociation of calcium. *Nature* **418,** 605–611
28. Olesen, C., Picard, M., Winther, A.-M., Gyrup, C., Morth, J. P., Oxvig, C., Møller, J. V., and Nissen, P. (2007) The structural basis of calcium transport by the calcium pump. *Nature* **450,** 1036–1042
29. Wictome, M., Michelangeli, F., Lee, A. G., and East, J. M. (1992) The inhibitors thapsigargin and 2,5-di(tert-butyl)-1,4-benzohydroquinone favour the E2 form of the Ca^{2+},Mg^{2+}-ATPase. *FEBS Lett.* **304,** 109–113
30. Sagara, Y., Wade, J. B., and Inesi, G. (1992) A conformational mechanism for formation of a dead-end complex by the sarcoplasmic reticulum ATPase with thapsigargin. *J. Biol. Chem.* **267,** 1286–1292
31. Fortea, M. I., Soler, F., and Fernandez-Belda, F. (2001) Unravelling the interaction of thapsigargin with the conformational states of Ca^{2+}-ATPase from skeletal sarcoplasmic reticulum. *J. Biol. Chem.* **276,** 37266–37272
32. Møller, J. V., Olesen, C., Winther, A.-M., and Nissen, P. (2010) The sarcoplasmic Ca^{2+}-ATPase: design of a perfect chemi-osmotic pump. *Q. Rev. Biophys.* **43,** 501–566
33. Gerdes, U., and Møller, J. V. (1983) The Ca^{2+} permeability of sarcoplasmic reticulum vesicles. II. Ca^{2+} efflux in the energized state of the calcium pump. *Biochim. Biophys. Acta* **734,** 191–200
34. Levy, D., Seigneuret, M., Bluzat, A., and Rigaud, J. L. (1990) Evidence for proton countertransport by the sarcoplasmic reticulum Ca^{2+}-ATPase during calcium transport in reconstituted proteoliposomes with low ionic permeability. *J. Biol. Chem.* **265,** 19524–19534
35. Bonilla, M., Nastase, K. K., and Cunningham, K. W. (2002) Essential role of calcineurin in response to endoplasmic reticulum stress. *EMBO J.* **21,** 2343–2353
36. Lotem, J., and Sachs, L. (1998) Different mechanisms for suppression of apoptosis by cytokines and calcium mobilizing compounds. *Proc. Natl. Acad. Sci. U.S.A.* **95,** 4601–4606
37. Chua, B. T., Guo, K., and Li, P. (2000) Direct cleavage by the calcium-activated protease calpain can lead to inactivation of caspases. *J. Biol. Chem.* **275,** 5131–5135
38. Lankiewicz, S., Marc Luetjens, C., Truc Bui, N., Krohn, A. J., Poppe, M., Cole, G. M., Saido, T. C., and Prehn, J. H. (2000) Activation of calpain I converts excitotoxic neuron death into a caspase-independent cell death. *J. Biol. Chem.* **275,** 17064–17071
39. Muruganandan, S., and Cribb, A. E. (2006) Calpain-induced endoplasmic reticulum stress and cell death following cytotoxic damage to renal cells. *Toxicol. Sci.* **94,** 118–128
40. Kroemer, G. (2015) Autophagy: a druggable process that is deregulated in aging and human disease. *J. Clin. Investig.* **125,** 1–4
41. Broegger Christensen, S., Kjoeller Larsen, I., Rasmussen, U., and Christophersen, C. (1982) Thapsigargin and thapsigargicin, two histamine liberating sesquiterpene lactones from *Thapsia garganica*. X-ray analysis of the 7,11-epoxide of thapsigargin. *J. Org. Chem.* **47,** 649–652
42. Jakobsen, C. M., Denmeade, S. R., Isaacs, J. T., Gady, A., Olsen, C. E., and Christensen, S. B. (2001) Design, synthesis, and pharmacological evaluation of thapsigargin analogues for targeting apoptosis to prostatic cancer cells. *J. Med. Chem.* **44,** 4696–4703
43. Møller, J. V., and Olesen, C. (2016) Preparation of Ca^{2+}-ATPase1a enzyme from rabbit sarcoplasmic reticulum. *Methods Mol. Biol.* **1377,** 11–17